

AD-A173 719

THERMAL ASPECTS OF FUTURE SPACECRAFT THERMAL MANAGEMENT 1/1

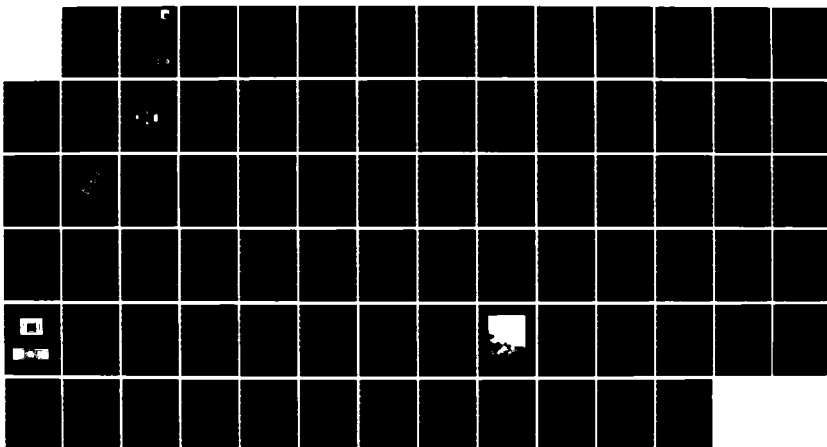
SYSTEMS(U) MISSOURI UNIV-ROLLA DEPT OF MECHANICAL AND
AEROSPACE ENGINEER. J W SHEFFIELD ET AL. JUL 86

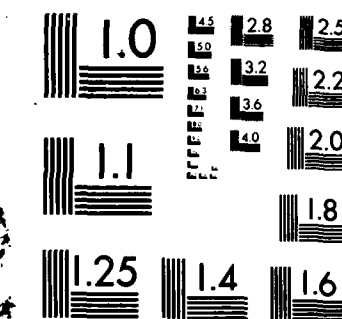
UNCLASSIFIED

AFWAL-TR-86-2021 F33615-81-C-2058

F/G 22/2

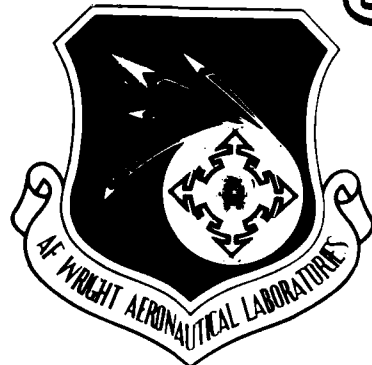
NL





MICROCOPY RESOLUTION TEST CHART
NATIONAL BUREAU OF STANDARDS 1963-A

AFWAL-TR-86-2021



THERMAL ASPECTS OF FUTURE SPACECRAFT THERMAL MANAGEMENT SYSTEMS

AD-A173 719

John W. Sheffield, Ph.D.
Raghav P. Kher

Mechanical and Aerospace Engineering
University of Missouri-Rolla
Rolla, MO 65401

July 1986

INTERIM REPORT FOR PERIOD JANUARY 1984 - OCTOBER 1985

APPROVED FOR PUBLIC RELEASE; DISTRIBUTION UNLIMITED

DTIC FILE COPY

DTIC
ELECTED
NOV 05 1986
S E D

AERO PROPULSION LABORATORY
AIR FORCE WRIGHT AERONAUTICAL LABORATORIES
AIR FORCE SYSTEMS COMMAND
WRIGHT-PATTERSON AIR FORCE BASE, OHIO 45433-6563

410118 SH

86 11 002

UNCLASSIFIED

SECURITY CLASSIFICATION OF THIS PAGE

REPORT DOCUMENTATION PAGE

1a. REPORT SECURITY CLASSIFICATION UNCLASSIFIED		1b. RESTRICTIVE MARKINGS A173 719										
2a. SECURITY CLASSIFICATION AUTHORITY		3. DISTRIBUTION/AVAILABILITY OF REPORT Approved for public release: distribution unlimited.										
2b. DECLASSIFICATION/DOWNGRADING SCHEDULE												
4. PERFORMING ORGANIZATION REPORT NUMBER(S)		5. MONITORING ORGANIZATION REPORT NUMBER(S) AFWAL-TR-86-2021										
6a. NAME OF PERFORMING ORGANIZATION University of Missouri-Rolla	6b. OFFICE SYMBOL (If applicable)	7a. NAME OF MONITORING ORGANIZATION Aero Propulsion Laboratory (AFWAL/POOS)										
6c. ADDRESS (City, State and ZIP Code) Mechanical & Aerospace Engineering Rolla, MO 65401		7b. ADDRESS (City, State and ZIP Code) Air Force Wright Aeronautical Laboratories Wright-Patterson AFB, OH 45433										
8a. NAME OF FUNDING/SPONSORING ORGANIZATION	8b. OFFICE SYMBOL (If applicable)	9. PROCUREMENT INSTRUMENT IDENTIFICATION NUMBER F33615-81-C-2058 Task 11										
8c. ADDRESS (City, State and ZIP Code)		10. SOURCE OF FUNDING NOS <table border="1"><tr><th>PROGRAM ELEMENT NO.</th><th>PROJECT NO.</th><th>TASK NO.</th><th>WORK UNIT NO.</th></tr><tr><td>62203F</td><td>3145</td><td>19</td><td>49</td></tr></table>		PROGRAM ELEMENT NO.	PROJECT NO.	TASK NO.	WORK UNIT NO.	62203F	3145	19	49	
PROGRAM ELEMENT NO.	PROJECT NO.	TASK NO.	WORK UNIT NO.									
62203F	3145	19	49									
11. TITLE (Include Security Classification) THERMAL ASPECTS OF FUTURE SPACECRAFT THERMAL MANAGEMENT SYSTEMS												
12. PERSONAL AUTHOR(S) Sheffield, John William												
13a. TYPE OF REPORT INTERIM	13b. TIME COVERED FROM 84/1/1 to 85/10/1	14. DATE OF REPORT (Yr., Mo., Day) July 1986	15. PAGE COUNT 79									
16. SUPPLEMENTARY NOTATION												
17. COSATI CODES <table border="1"><tr><th>FIELD</th><th>GROUP</th><th>SUB. GR.</th></tr><tr><td>22</td><td>02</td><td></td></tr><tr><td>10</td><td>03</td><td></td></tr></table>		FIELD	GROUP	SUB. GR.	22	02		10	03		18. SUBJECT TERMS (Continue on reverse if necessary and identify by block number) I. Thermal Energy Storage; II. Phase Change Material; III. Spacecraft Thermal Management Systems.	
FIELD	GROUP	SUB. GR.										
22	02											
10	03											
19. ABSTRACT (Continue on reverse if necessary and identify by block number) This report primarily addresses the conceptual design of spacecraft thermal management systems (SCTMS) and their components in order to provide a basis for the development and implementation of future technologies. In the analysis, the components of the SCTMS include the following: heat pipes, latent thermal energy storage materials, radiators and other thermal structures. The design problem becomes one of selecting a combination of these components subject to both spacecraft mission and launch requirements. To assist in this design process, a knowledge-based software has been developed in the artificial intelligence programming language, PROLOG. This software serves as a design assistant for the development of SCTMS. It supports facilities such as database retrieval, numerical computation, and logical decision making. With these features one can automatically consider all relevant combinations of components, technologies, and materials for the design problem. The goal has been to duplicate, wherever possible, the decision processes of an experienced designer by putting significant decision making, search, and retrieval facilities at his disposal (see other side).												
20. DISTRIBUTION/AVAILABILITY OF ABSTRACT <input checked="" type="checkbox"/> UNCLASSIFIED/UNLIMITED <input type="checkbox"/> SAME AS RPT. <input type="checkbox"/> DTIC USERS <input type="checkbox"/>		21. ABSTRACT SECURITY CLASSIFICATION UNCLASSIFIED										
22a. NAME OF RESPONSIBLE INDIVIDUAL V. J. Van Griethuysen		22b. TELEPHONE NUMBER (Include Area Code) (513) 255-6241	22c. OFFICE SYMBOL AFWAL/POOS-3									

19. ~~Other~~ her disposal.

~~The~~ other objectives of this investigation were to determine the capabilities of the phase change materials (PCMs) selected by the knowledge-based system. Tests were carried to evaluate properties and thermal behavior of a PCM in pellet form. Two types of PCMs demonstrated potential for SCTMS were calcium chloride hexahydrate and the form stable crystalline polymer, high density polyethylene.

X

FOREWORD

The information presented in this report was generated during the performance of the task 011 of CONTRACT No. F33615-81-C-2050/ SB5448-81-C-0100. The technical work was carried out at the University of Missouri-Rolla, Department of Mechanical and Aerospace Engineering.

Dr. John W. Sheffield was the principal investigator of the program. Raghav P. Kher was the graduate student supported by this contract. This is an interim report which presents the results generated during the period of 1 January 1984 to 1 October 1985. The program was sponsored by the Aeronautical Systems Division of the Air Force with Ms. V. J. Van Griethuysen of the Power Technology Branch at the Aero Propulsion Laboratory (AFWAL/POOS) serving as the technical monitor.

Accession For	
NTIS GRA&I	<input checked="" type="checkbox"/>
DTIC TAB	<input type="checkbox"/>
Unannounced	<input type="checkbox"/>
Justification	
By	
Distribution/	
Availability Codes	
Dist	Avail and/or Special
A-1	



TABLE OF CONTENTS

	Page
I INTRODUCTION	1
II BACKGROUND	6
A. PHASE CHANGE MATERIALS	6
B. HEAT PIPES	16
C. RADIATORS	18
D. ARTIFICIAL INTELLIGENCE	19
III PROPOSED CONCEPT	22
A. MODELING OF THE PROPOSED SYSTEM	22
B. KNOWLEDGE-BASED SYSTEM	29
IV EXPERIMENTAL PROGRAM	42
A. FUSIBLE PELLET CONCEPT	43
B. HEAT TRANSFER EXPERIMENTS	43
C. DESIGN ANALYSIS	45
V EXPERIMENTAL RESULTS	48
VI CONCLUSIONS AND RECOMMENDATIONS	62
BIBLIOGRAPHY	66

LIST OF ILLUSTRATIONS

Figure	Page
1 Philosophy of Design Concepts	3
2 Steps in the Overall Thermal Control Design Process	4
3 Microencapsulated PCM	9
a) Cross-Section	9
b) Stacking Arrangement	9
4 Fluidized Microencapsulated PCM Concept	11
5 Moving PCM Concept	13
6 Heat Pipe Concept	14
7 Heat Pipe	17
8 Design Aspects of the Proposed Concept	23
9 Baseline Concept	24
a) Conceptual Heat Rejection System	24
b) Heat Flow	24
10 Design Assistant Flow Chart	31
11 Design Assistant Levels of Knowledge	32
12 Family of Phase Change Materials	34
13 PCM Database	37
14 Proposed Heat Pipe Database	41
15 Heat Exchanger	44
16 Phase Change of HDPE Pellet	44
17 Cylinder of HDPE after Multiple Phase Change Cycling . . .	52
18 Pressure Drop vs. L/D Ratio for Cylindrical Bed of HDPE . .	55
19 Pressure Drop vs. L/D Ratio for Cylindrical Bed of $\text{CaCl}_2 \cdot 6\text{H}_2\text{O}$	55
20 Pressure Drop vs. L/D Ratio for Rectangular Bed of HDPE . .	57

21	Pressure Drop vs. L/D Ratio for Rectangular Bed of $\text{CaCl}_2 \cdot 6\text{H}_2\text{O}$	57
22	Present Experimental Setup	58
23	Fluid Temperature vs. Time for Flow Rate of 0.2 gpm	59
24	Fluid Temperature vs. Time for Flow Rate of 0.3 gpm	59
25	Fluid Temperature vs. Time Curves for Flow Rate of 0.4 gpm	60
26	Mass Fraction vs. Time Curves for Different Flow Rates	60
27	Proposed Experimental Setup	64

LIST OF TABLES

Table	Page
I Emerging Heat Pipe Technologies	1
II Desired Characteristics of Latent Thermal Storage Systems .	7
III Desired Properties of PCMs	35
IV Phase Change Materials Considerations	36
V Parameters Considered in the Analysis	40
VI Properties of PCM Pellets	47
VII HDPE Porosity vs. Temperature and Pressure	50
VIII $\text{CaCl}_2 \cdot 6\text{H}_2\text{O}$ Porosity vs. Pressure	50

NOMENCLATURE

A_F = Cross sectional area of the fluid voids, m^2 .
 A_s = Surface area of the spherical pellets, m^2 .
 Bi = Biot Number
 C = Specific heat at constant pressure
 CA = Capacity of the component, Watt- m
 D_h = Hydraulic diameter of the packed bed, m .
 D_s = Diameter of spherical pellets, m .
 f = Frictional factor
 g = Gravity constant, m/sec^2 .
 G = Specific weight, Watt/kg.
 h = Convective heat transfer coefficient, Watt/ $\text{m} \cdot ^\circ\text{C}$.
 H = Latent heat of fusion of the phase change material, kJ/kg .
 k = Thermal conductivity, Watt/ $\text{m} \cdot ^\circ\text{C}$.
 L = Length of the component, m .
 M = Mass, kg .
 n = Number of cycles of the periodic heat rejection load
 Δp = Pressure drop, kPa .
 N = Number of components
 q = Heat flux, Watt/ m^2 .
 Q = Rate of heat flow, Watt.
 R = Characteristic thickness, m .
 Re = Reynolds Number
 Ste = Stefan Number
 t = Time, sec.
 t_p = Time of the peak heat load, sec.
 T = Temperature, $^\circ\text{C}$.
 T = Temperature difference between the pellet and the fluid, $^\circ\text{C}$.

U = Coefficient of heat transfer, Watt/m².°C.

V = Volumetric flow rate, m³/sec.

X = Fraction of PCM melted

Greek

τ = Time required to melt one pellet layer of PCM, sec.

ϵ = Porosity

ρ = Mass density, kg/m³.

μ = Viscosity, kg/m.sec.

δ = Length that the fluid flows during the time for one pellet to melt, m.

Subscript

A = Average

c = Condenser

e = Evaporator

h = Heat Pipe

p = Phase Change Material

r = Radiator

LIST OF ACRONYMS

AI	Artificial Intelligence
HDPE	High Density Polyethylene
HTF	Heat Transfer Fluid
LHTES	Latent Heat Thermal Energy Storage
LISP	LISt Processing language
NASA	National Aeronautics and Space Administration
PROLOG	PROgramming in LOGic
PCM	Phase Change Material
SCTMS	SpaceCraft Thermal Management System
TG-DTA	Thermogalvanometry-Differential Thermal Analysis

I. INTRODUCTION

The reliability of a spacecraft can be enhanced greatly if its dependence upon power and endurance of moving parts is minimized. In reviewing the projections of future spacecraft power, life and mission requirements that are currently established, the thermal management of spacecraft is seen as an important issue in the overall design of the spacecraft system. Future spacecraft thermal management systems (SCTMS) will require advanced technologies in order to achieve the desired weight, size and life goals. These technologies might include high-capacity heat pipes, phase change materials (PCMs), and deployable radiator panels. High-capacity heat pipe technologies offer opportunities to customize isothermal panel design and allow deployment of additional thermal control surfaces. The emerging two-phase heat pipe technologies [1] include axial groove, monogroove, capillary pumped, and mechanically pumped loop configurations. The heat transport capacity of these heat pipes are shown in Table I.

Table I. Emerging Heat Pipe Technologies

TECHNOLOGY	CAPACITY [kW m]
Axial Groove (current)	0.25 - 1.0
Monogroove (current/projected)	25.0 - 100.0
Capillary Pumped (projected)	250.0 - 1000
Mechanically Pumped (projected)	25,000.0

Reviewing earlier developments of spacecraft technology such as the efforts sponsored by NASA (National Aeronautics and Space Administration) to develop PCM thermal control devices, passive thermal control systems were shown to be feasible and test results showed that PCM systems could reduce onboard equipment temperature fluctuations by at least 75% compared to unprotected spacecraft systems [2]. Basically, this earlier passive thermal management system concept was to sandwich the PCM between the equipment to be

controlled and the outer radiating surface of the satellite. A recent paper [3] investigated the sensitivity of the future SCTMS weight to the choice of PCM. The candidate PCMs can be classified as form stable polymers, encapsulated salt hydrates, paraffins and eutectic alloys.

Thermal management of future spacecraft will introduce many challenging design requirements. The thermal control, heat storage, heat transport, and heat rejection represent a set of major design problems when the mission constraints of large thermal loads are included. One of the more challenging thermal design requirements is the capability to handle both large and pulsed thermal loads. During and immediately following burst power conditions, large thermal loads must be removed from the source and rejected in some manner that minimizes the overall burden on the total system. The application of PCM appears to be an attractive choice [4]. The design of a SCTMS requires the determination of a large number of variables and their interdependence, including the integration of both mission and launch payload requirements. The comparison of conceptual designs requires system studies of configuration, thermal structures and subsystems. Figure 1 gives an example of the philosophy of design concepts for SCTMS. Figure 2 shows the steps in the overall thermal control design process [5].

It has become clear to the designers of SCTMS that significant reduction in the overall weight of space power systems can be achieved through the use of advanced radiator concepts, such as modular heat pipe panels, pumped fluid loop, deployable and liquid droplet. The variable conductance heat pipe thermal control systems can provide near isothermal conditions without moving parts and are finding increasing acceptance. The critical element in a deployable radiator design is the thermal contact of the joints. A flexible heat pipe is an excellent candidate for this application.

PHILOSOPHY OF DESIGN CONCEPTS

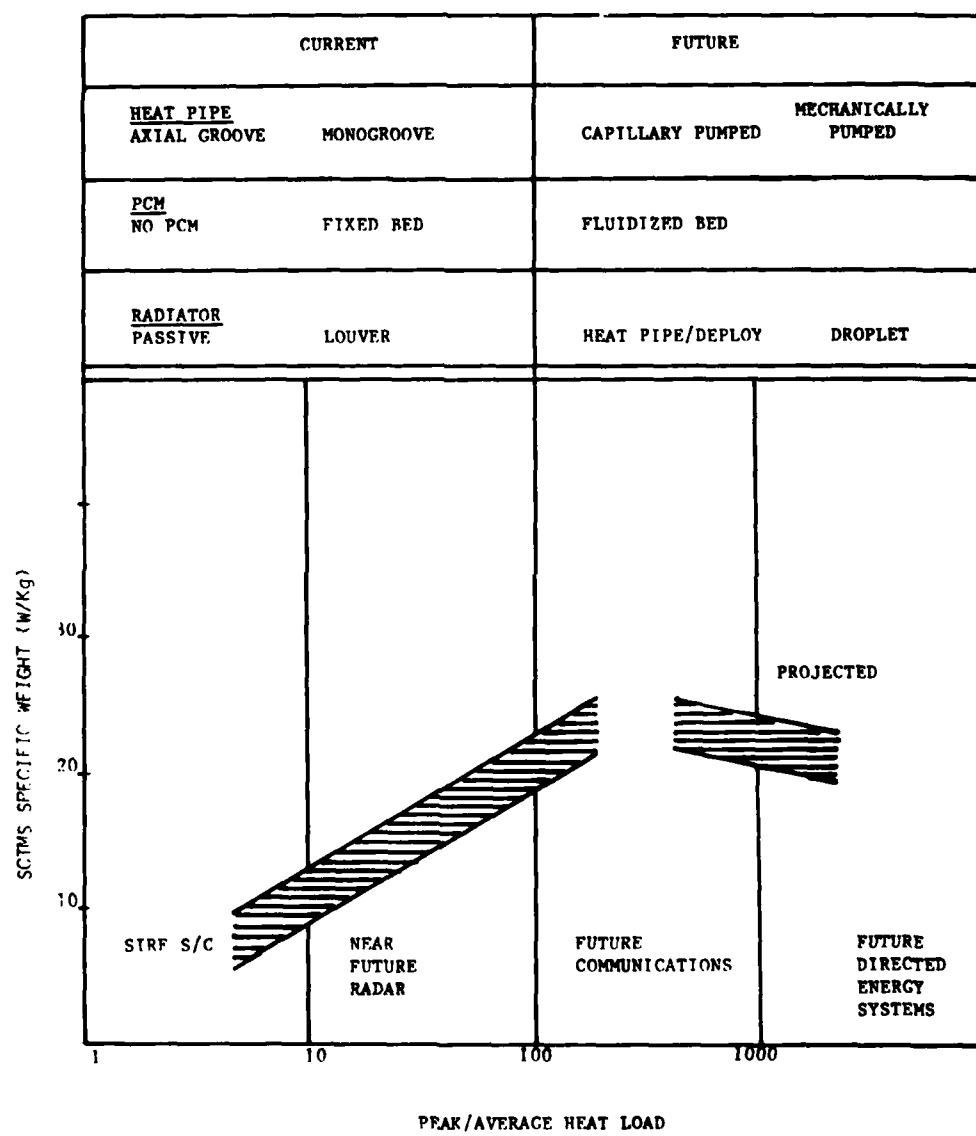


Figure 1. Philosophy of Design Concepts

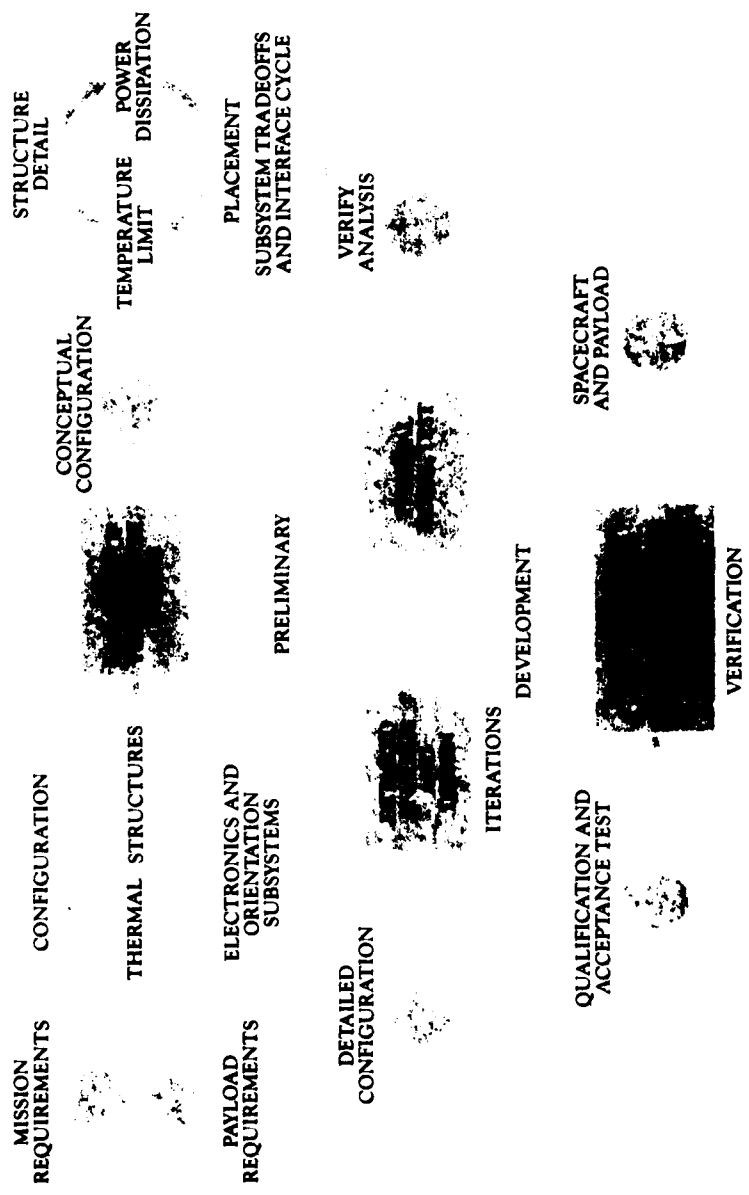


Figure 2. Steps in the Overall Thermal Control Design Process

Recently, as a part of an investigation 'Weight Characteristics of Future Spacecraft Thermal Management Systems' [6] sponsored by Air Force Wright Aeronautical Laboratories' Power Technology Branch, a SCTMS concept incorporating a PCM into a variable conductance heat pipe was explored. This concept of PCM microspheres allows for maximized surface to volume ratio and very rapid charging and discharging of thermal load. The microspheres have an additional potential of acting as a wicking material for condenser of heat pipes making this concept very promising.

The weight characteristics of future spacecraft thermal management systems have been discussed in a recent paper [3]. Performance parameters include the peak thermal load, the peak to average thermal load ratio and the length of the peak thermal load. In addition, the sensitivity of SCTMS weight to the choice of PCM was determined via a heat of fusion parametric analysis. As an ongoing research task, this report includes extensive literature survey covering different concepts for SCTMS, and hardware requirements of their applications. The first few pages of this report summarizes different aspects considered before choosing the heat pipe/PCM concept for current investigation. Detailed laboratory tests on different PCMs were done and a latent thermal energy storage unit was built and tests were carried out to determine the performance of the unit.

To assist in the design process, a knowledge-based system has been developed in a current artificial intelligence programming language, PROLOG (Programming in Logic) [7]. This software serves as a design assistant for the development of SCTMS. It supports facilities such as database retrieval, numeric computation and logical decision making. These features allow one to automatically consider all relevant combinations of components, technologies and materials for the design problem.

II. BACKGROUND

A. PHASE CHANGE MATERIALS

A promising thermal control concept not yet widely employed in the space is the use of Phase Change Materials (PCMs). These materials have extremely long lifetime, and could be used to maintain a relatively constant temperature of an electronic device or to store heat energy for later release. The latent heat-of-fusion concept, that is storing and recovering heat through the solid-liquid phase change process, has two important advantages: (1) the latent heat of fusion of most materials is much higher than their sensible heat, thus requiring much smaller mass of storage medium for storing/recovering a given quantity of thermal energy and (2) the thermal storage process occurs at nearly constant temperature, which is typically desirable for efficient operation of most thermal systems. A good understanding of the heat transfer process involved is essential for accurately predicting the thermal performance of the system and for avoiding costly system design.

The heat transfer and design aspects of Latent Heat Thermal Energy Storage (LHTES) systems are more complex than those in sensible systems due to: (1) nonlinearity of the problem resulting from the motion of the solid-liquid interface during phase change process; (2) uncertainty of the interface thermal resistance between the container wall (or transport fluid channel) and the solid PCM; (3) volume change of phase change (upon shrinkage, void cavities may arise in the solid and reduce the heat transfer process significantly); and (4) the presence and configuration of voids in solids which may also introduce the complex phenomena of natural convection and internal radiation, particularly at higher temperatures. There are few examples of technical data available on the latter four problem areas mentioned that would be applicable to the design of latent heat thermal energy

storage systems (LHTES). The following pages give a few design concepts for LHTES. Table II gives the desired characteristics of latent heat thermal storage systems.

Table II. Desired Characteristics of Latent Thermal Storage System

1. Compact: Large heat storage capacity per unit mass volume.
2. High storage efficiency: High thermal conductivity.
3. Heat storage medium with suitable properties in operating temperature range.
4. Capacity to charge and discharge with the largest heat input/output rates but without large temperature gradients.
5. Ability to undergo large number of charging/discharging cycles without loss in performance and storage capacity.
6. Small self-discharging rate i.e., negligible heat losses to surroundings.
7. Inexpensive

1. Micro-encapsulated PCM Concept: In this concept, relatively large quantities of PCM are encapsulated with thin layers of containment material (steel) which deform to accommodate volumetric changes associated with change of phase [8]. Relatively small quantities of containment material would be required, since the thickness would have to be small to minimize bending stress. One such configuration, consisting of long 'plank' shaped blocks of PCM is shown in Fig. 3. The plank cross section would be essentially rectangular when the PCM is at maximum density in solid state. The edges would be relatively stiff and the top and bottom surfaces would bulge outward as indicated to accommodate volumetric expansion associated with melting. The planks would be stacked in a pressure vessel as shown in Fig. 3-B, with the gap regions provided for liquid heat transfer fluid flow. The gap height

should be adjusted by design of the plank edge shape to be as small as possible consistent with allowable flow pressure drops and required film coefficient for heat transfer. High overall packing density is desirable to minimize pressure vessel size and cost.

The principal disadvantage of this concept is the cost of the required pressure vessels. An intermediate low pressure circulating loop might be considered to eliminate the pressure vessels, but the cost of the heat exchangers for such a loop would probably be comparable to the cost of the equivalent boiler capacity being replaced. A better approach primarily suited to very large thermal energy storage applications.

2. Intermediate Pumped Loop: The use of a low pressure intermediate liquid metal circulating is an alternative variation on the base line tube/shell PCM concept. The low pressure would permit significant reductions in wall thickness for the tubes and shell domes. This would be off-set to some extent by the cost of heat exchangers, pumps, and piping for the liquid metal loop. Heat exchanger bypass lines could be provided in the loop with bypass flow varied to compensate for variable thermal resistance within the PCM associated with movement of liquid solid interface. This bypass control should result in more uniform steam and water outlet temperatures, however, it might experience reduced reliability.

3. Fluidized Encapsulated PCM: Micro-encapsulating the PCM, using particle sizes comparable to that of pulverized coal (e.g. 50-100 μ) is attractive because it eliminates the need for heat exchangers though this may be off-set by encapsulation cost [8]. This concept is illustrated in Fig. 4 using a one bin empty system. For heat storage, cold encapsulated PCM is drawn from a filled bin, entrained by carrier steam, and deposited hot in the

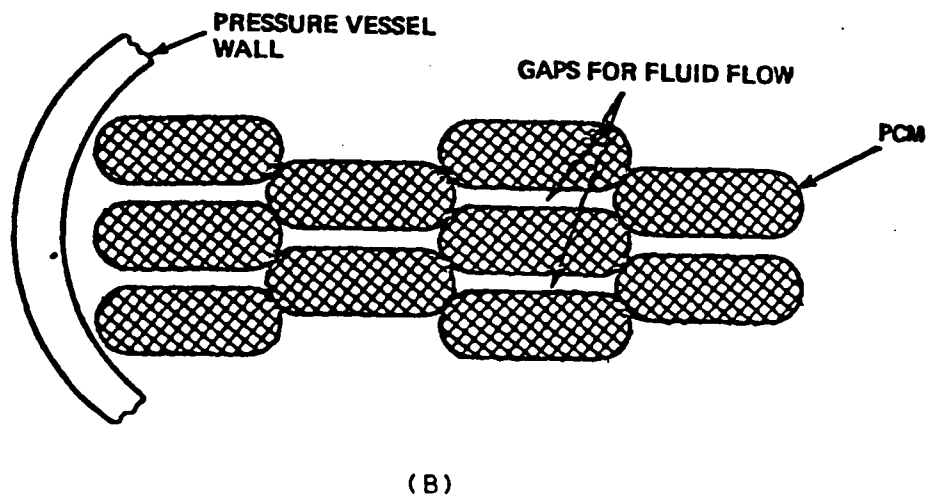
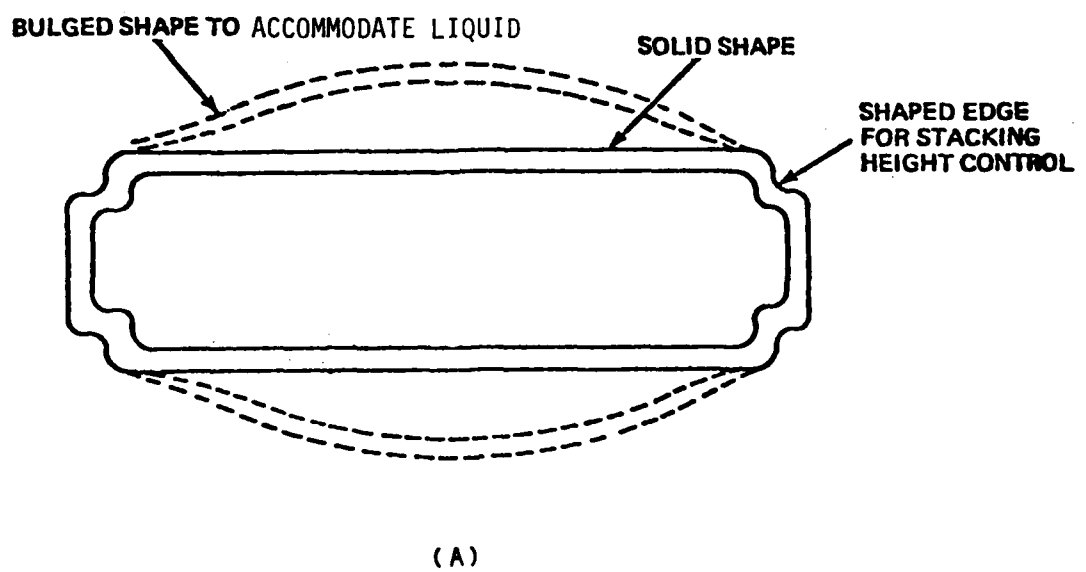


Figure 3. Microencapsulated PCM a) Cross-Section
b) Stacking Arrangement

next (empty) bin. One bin is depleted as the other fills. When full, valves are adjusted to repeat the process of taking PCM from another cold bin and putting it into the previously emptied bin. Bins would be large enough to permit particle settling, with the carrier fluid drawn off at the top. For heat removal, the carrier fluid would be liquid water in the feedwater heating case, or liquid evolving to steam in auxiliary power cycle case. As with the other PCM concepts, several PCMs with different melt temperatures might be used, using separate sets of bins for each PCM, each based on one bin empty concept. The micro-encapsulated PCM - system would differ from a pulverized coal system in having to take full cycle pressure. Provision for bin-to-bin venting would be required to minimize pressure variations during PCM transfer.

Also, it would be desirable to have following mass flow rate:

$$m_w (h_{sw}) = m_p (H + h_{sp})$$

where h_{sw} = sensible heat of water

h_{sp} = sensible heat of PCM

m_w = mass of water

so that all the heat transfer for each PCM could be accomplished with a single entrainment. Then sensible energy storage would be greater for microencapsulated PCM than for other concepts, since the PCM would quickly approach the carrier fluid temperature with negligible exit temperature differences. This permits smaller quantities of PCM while all systems will have containment material associated with sensible heat storage, the mass of such material may be somewhat larger for microencapsulated than it would be for other concepts.

From a safety point of view, microencapsulation presents two problems, failure of encapsulating shells and failure of the pressurized bins. Encapsulated shell failure would release small quantities of PCM which could react with carrier fluid, with some particle agglomeration probable. Use of

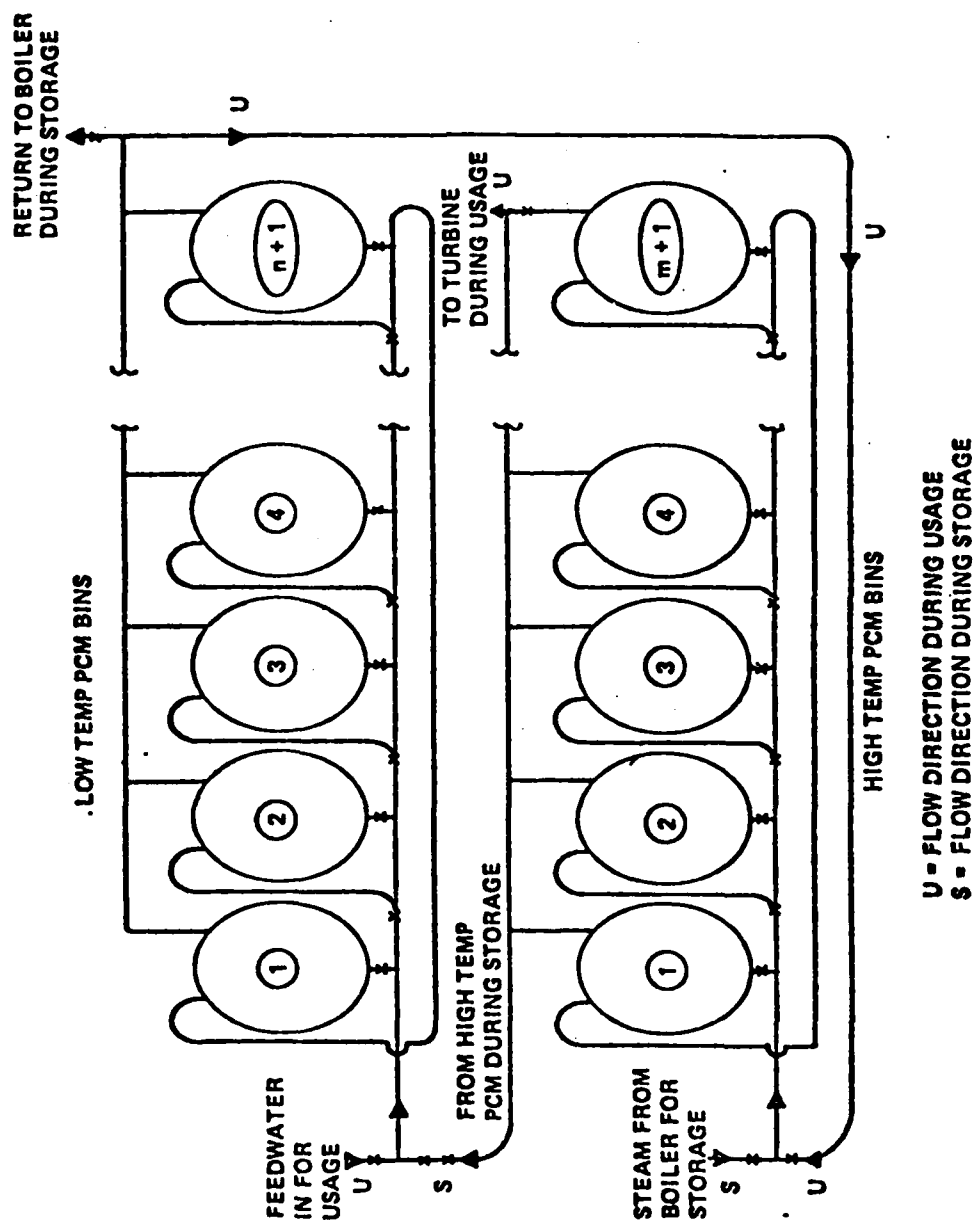


Figure 4. Fluidized Microencapsulated PCM Concept

relatively coarse mesh screen or periodic bin cleaning might be required. Bin structural failure, as with any pressure vessel, is a serious problem, but only the void volume in the bin would contain high pressure fluid capable of contributing work of expansion. Also, the encapsulated particles should present somewhat less hazard than bulk PCM.

Major drawbacks associated with materials and processes for encapsulation of microencapsulated are not completely known. If encapsulated PCM could be provided at moderate cost (\$0.5/Kg), the system would be more attractive but would still result in added cost for pressure vessel and high pressure valves [8]. Development of hardware and flow relations associated with handling of microencapsulated PCM are not trivial problems but appear soluble with straight forward engineering effort.

4. Moving PCM Concept: The moving PCM concept attempts to minimize required heat transfer surface area by eliminating most of the thermal resistance within the PCM [8]. The liquid solid interface is always kept close to the heat transfer surface. This concept is illustrated schematically in Fig. 5. During usage, liquid PCM flow through slit nozzles on to rotating drums. The heat sink fluid flows through the drums, cooling the surfaces and freezing the PCM. The solid PCM is scrapped off after making a partial rotation, falling into a storage bin. For heat storage, the source fluid is fed through heat exchangers located at the bottom of the bin which has a pitched floor arranged so that the PCM melts off as it drains. The liquid PCM is pumped into an insulated tank until needed for part of the cycle. Potential problems associated with liquid PCM pumping are recognized, such as flow blockage in the pumps due to PCM solidification. This concept was originally

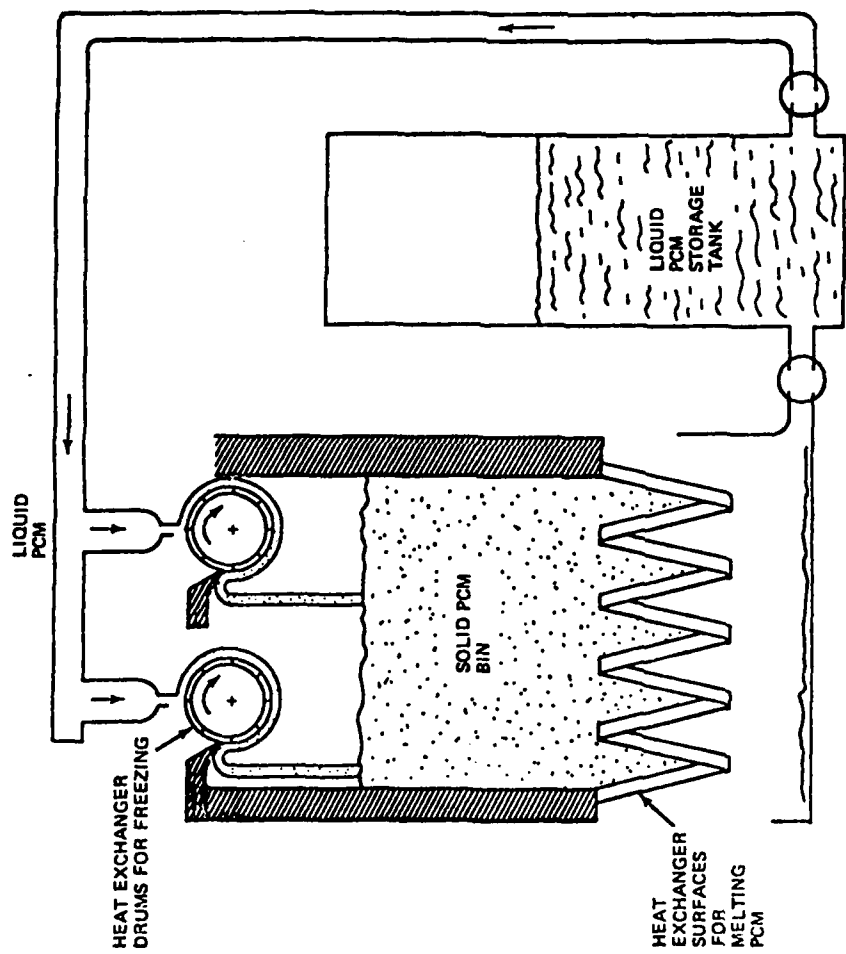
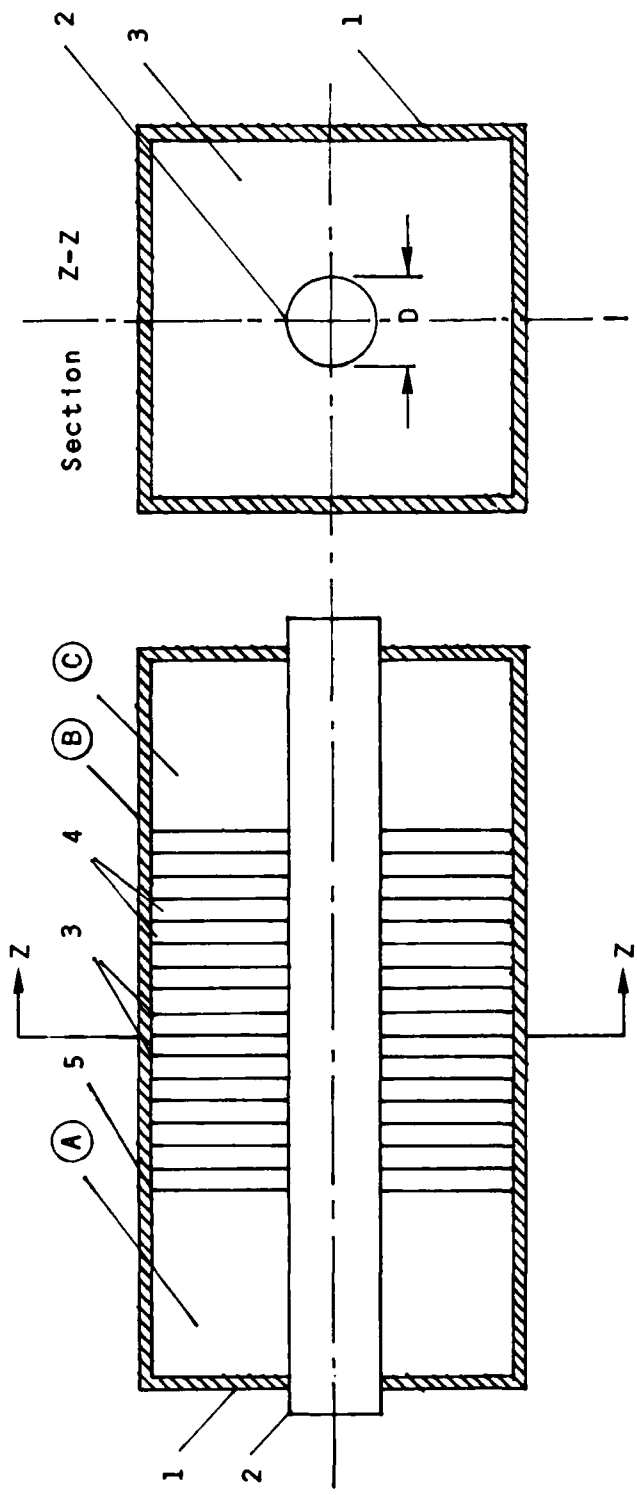


Figure 5. Moving PCM Concept



1	Container
2	Heat Pipe
3	Fins
4	Storage Medium
5	Separation Walls

(A)	Heat Source Region
(B)	Storage Chamber
(C)	Heat Sink Region

Figure 6. Heat Pipe Concept

conceived as a terrestrial design, however, a closed loop pumped system could be considered for space designs.

5. Heat Pipe Concept : This is a new type of a passive heat exchanger presently under development. The major advantages offered by this type of heat exchanger are its modular design and flexibility in application in that it can equally be used with liquid or air as heat transfer medium.

Figure 6 shows a schematic of a single heat exchanger module essentially compromised of a container (1) of square cross section provided with a heat pipe (2) along its longitudinal axis [9]. The container as well as heat pipe are divided into three regions - region A, B and C in Fig. 6 by separation walls (5). One of the regions B, is filled with a heat of fusion type material and is called storage chamber. The remaining two regions A and C are in contact with fluid flowing through the heating loops, and are termed as heat source or heat sink regions respectively.

The heat pipe length within the storage chamber is provided with closely and equally spaced square fins of large cross sections (3), made from a material of high thermal conductivity, i.e. aluminum. The storage medium (4) fills the free volume between the fins. Thus embedded within the storage medium, the fins compensate for its generally poor thermal conductivity and simultaneously insure small heat flow paths within LHTES system.

The use of the heat pipe offers several advantages and increases flexibility in operation and application. Some of these are:

a. Additional heat exchangers are eliminated. Furthermore, the heat pipe length within the heat source and heat sink regions may be suitably finned depending on whether air or liquid is employed as heat transfer medium in these regions.

- b. The heat pipe transports heat under low temperature gradient so that almost isothermal heat source in contact with the fins and thermal storage medium within the storage chamber is attained.
- c. The heat flux transformation capability of the heat pipe can be utilized to give low heat flux densities within the storage chamber for large heat flow rates in heat source/sink sections.
- d. The heat pipe can operate unidirectionally as a thermal diode.

B. HEAT PIPES

The heat pipe is a device with an effective thermal conductance much higher than even the best heat conducting metal. This property makes it especially suited for space applications in which a large amount of heat must be transferred from one area to another, or when a stable 'isothermal' condition is required in an area subject to internal heat generation.

Figure 7 shows the basic concept for a standard heat pipe [5]. The heat pipe operates on the same principle as a reflux boiler, but depends upon the capillary action of a wick rather than gravity to return the condensed vapor from the heat radiator (condenser) to the heat source (evaporator).

The standard heat pipe has a fixed conductance and must therefore be designed to handle a constant and specific heat load. A later development, the variable conductance heat pipe, makes it possible to control the conductance as a function of temperature, which broadens considerably the applications for this highly efficient device. Variable conductance is achieved by means of a noncondensable gas contained at the condenser end of the heat pipe. This gas expands and contracts with changes in vapor temperature within the pipe, thus changing the effective condenser heat transfer area.

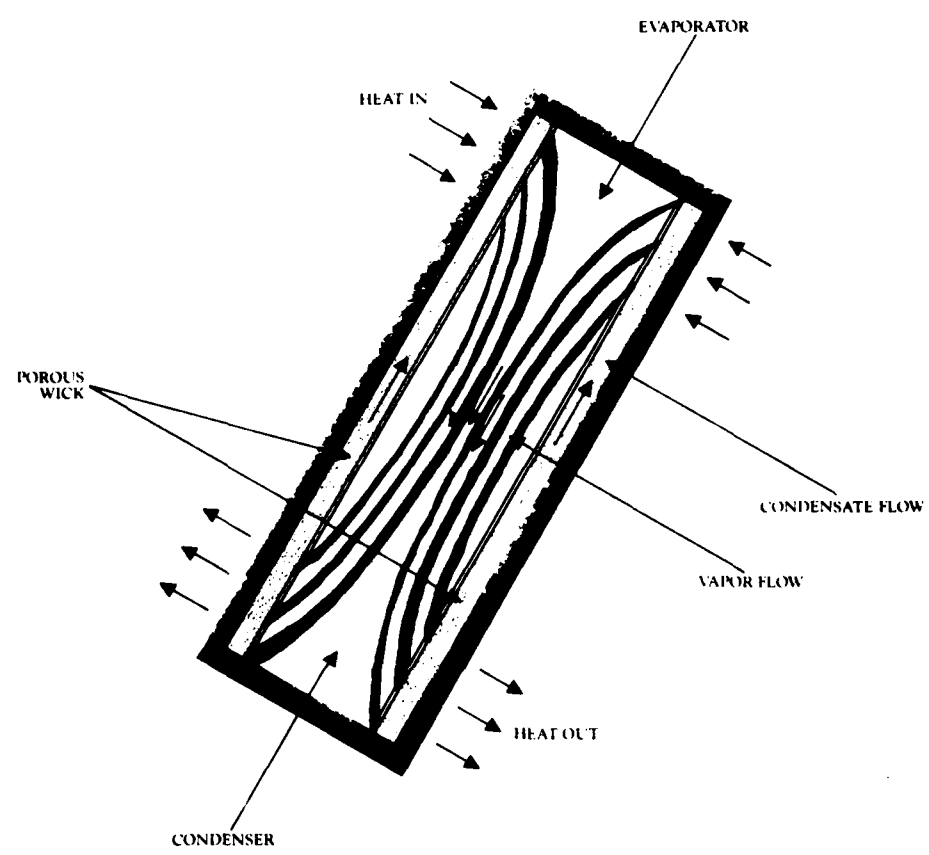


Figure 7. Heat Pipe

C. RADIATORS

In almost all advanced space projects, there are requirements to remove heat from space vehicles during very long periods of time. The only practical way of such continuous heat rejection from a system in an outer space environment is by radiation.

Radiators for space vehicle environmental control systems may be considered as low-temperature radiators; they are differentiated from high-temperature radiators in that the net heat rejection from low-temperature radiators is of the same order of magnitude as the heat flux incident upon the radiator from surrounding environment. In other words the radiator temperature is relatively low and is not greatly above the effective environment temperature. The distinguishing feature of low temperature radiators is that they depend to a large extent upon the spectrally-selective material used as a surface coating. This coating should have as high as an emissivity as possible and as low as possible absorptivity for solar radiation. The design of radiators requires knowledge of the heat transfer processes and thermal design, methods of meteoroid protection, fabrication, and reliability requirements for radiator components. Although the basic laws of radiant heat transfer are well known, the design of the actual hardware to be used in radiator systems for space vehicles is not well developed. One reason for this is that there are many severe criteria that must be met by space heat rejection systems. Among these criteria are low weight, high reliability, operation in vacuum environment of space, and the capability of continuous operation despite many possible collisions with meteoroid. The low weight and invulnerability to meteoroid collision are probably the most limiting specifications to be considered in radiator design.

D. ARTIFICIAL INTELLIGENCE

Definitions of the phrase 'artificial intelligence' (AI) vary widely from author to author, and a given author will tailor his or her definitions to his or her particular audience. Definitions made by AI researchers to their colleagues emphasize subtle points of philosophy, technology, and methodology. Definitions for a more general audience must give a more general characterization. Many definitions refer to the long term goals of artificial intelligence research to emulate human intellectual abilities. This may give a philosophical perspective on the domain but it may leave the impression that accounting and inventory programs are really artificial intelligence since they emulate, and in fact replace, humans that used to perform these functions. Hence, it is useful to identify the types of problems which have been the subject of AI research.

A recent paper [10] identifies three features of typical AI problems. These problems have been characterized, first of all, as combinatorially complex problems. The second feature of AI problems is that AI has been applied to problems for which no known 'solution process' exists. The only path to a solution may be through the application of 'general principles', 'rules of thumb', or 'educated guesses'. The problems are computationally so complex that it is impossible to ever find an optimal solution. In fact, the problems involve the consideration of so many factors that it may be impossible numerically to quantify the 'value' of a solution. It may only be possible to qualify a solution as good or bad, or qualify one solution as better or worse than another. Typically, AI problems are so hard, that just one satisfactory solution is valued.

AI is distinguished by the problems that it addresses and also the techniques and technology which it applies to those problems. Kempf [11] defines AI as a three stage problem solving technique to determine:

- a. All available knowledge that can be applied to the combinatorial complexity of the problem.
- b. Some representation for that knowledge.
- c. A methodology for applying that knowledge to the problem.

Of course this is a good problem solving methodology for any subject domain. For familiar, well defined engineering problems, the relevant knowledge is applied to equations and algorithms where the representation is often a FORTRAN program. This knowledge is then utilized by applying the program to a file of input data yielding an output file of solutions. However, as problems become more complex and less well defined, the relevant knowledge covers a spectrum of facts, decision rules, equations, and algorithms. As problems of representation become more complex, the problem of applying the knowledge becomes more difficult. For this reason most AI applications have been implemented in symbolic languages, such as LISP or PROLOG, which are more suitable for the representation of many different kinds of information and which can access and process that information in many different ways.

The first goal is to capture the expertise of a human researcher [12], and to emulate a methodology in the design of future SCTMS. When all of the potential design options are considered together in all of their combinations the number of potential designs becomes exponentially large. Instead the design process is far from that which we would call algorithmic. It involves a creative process of inventing a potential design, which is then further refined and modified according to many general principles. Finally, the solution must meet certain basic requirements. It may even be possible to characterize a design as good or bad, but so many factors must be considered that it is not clear what 'optimal' might mean.

Attempts to automate design processes is a relatively new endeavor in AI. Many other areas of AI have been the subject of years of ongoing research:

game playing, theorem proving, vision, natural language understanding, learning, diagnosis, etc., but engineering design poses some unique difficulties. A human designer brings a vast body of factual and experiential knowledge to bear on a design problem. The resulting design must of course satisfy certain requirements, but the number of satisfactory designs is unlimited. Hence, an AI system which emulates a human designer must have access to vast bodies of knowledge, it must have the capability to learn from its previous designs, and it must have very sophisticated mechanisms for focusing on a few candidate designs.

A recent work on automated design [10] gives some direction to implementation of automated design systems. The authors of that paper identify three classes of design problems:

- a. Class 1 is very creative, requires extensive knowledge and experience, and involves consideration of an unlimited number of solutions.
- b. Class 2 is generally routine, perhaps even repetitive, but it requires in most cases some inventiveness and creativity to resolve some aspects of the design.
- c. Class 3 follows a well-established, reasonably well understood design procedure. However the design problem is still 'hard' in the sense that there is still an effectively unlimited number of potential designs. Very specific knowledge and expertise is required to focus on a few candidate designs and develop them from initial concept through several stages of modification and refine ~

The authors of that paper proposed that the Class 3 design is within the reach of current AI technology and techniques. Since the design of future SCTMS is hardly a routine process, the first step of this research was to restrict the scope of the design problem. The work effort was focussed on a specific configuration (heat pipe, heat storage, radiator) where a system

which would substantially automate the process of selecting compatible components for the system, properly sizing them, and refining their characteristics was implemented.

III. PROPOSED CONCEPT

In this investigation a simplistic approach was used in the modeling of the SCTMS. The basic concept was to divide the system into the generic components for the thermal modelling. Figure 8 shows some design aspects to the proposed concept formulation. Figures 9a and 9b illustrated schematically the baseline concept. Three components were selected. They are the heat transport heat pipes, the thermal storage system using a phase change material and the space radiators. A transient thermal analysis was conducted to determine the response for pulsed thermal loads. The transient thermal analysis was the Lumped-System Analysis [13] where the spatial variation of temperature is neglected and the variation of the temperature of the component with respect to time is studied. In this method the geometry of the component is immaterial since the temperature is considered to be a function of time only, hence the analysis becomes very simple. A three-lump system was used to extend the study of the transients in a composite system consisting of the three different components. In the following analysis, we considered the three components of the SCTMS, i.e., heat pipe, PCM and radiator, to be lump masses having essentially uniform temperatures.

A. MODELING OF THE PROPOSED SYSTEM

1. Transient Thermal Analysis: The mathematical formulation of the problem depends on the number of lumps considered for the system analysis and on the type of boundary conditions for the heat transfer. In this analysis,

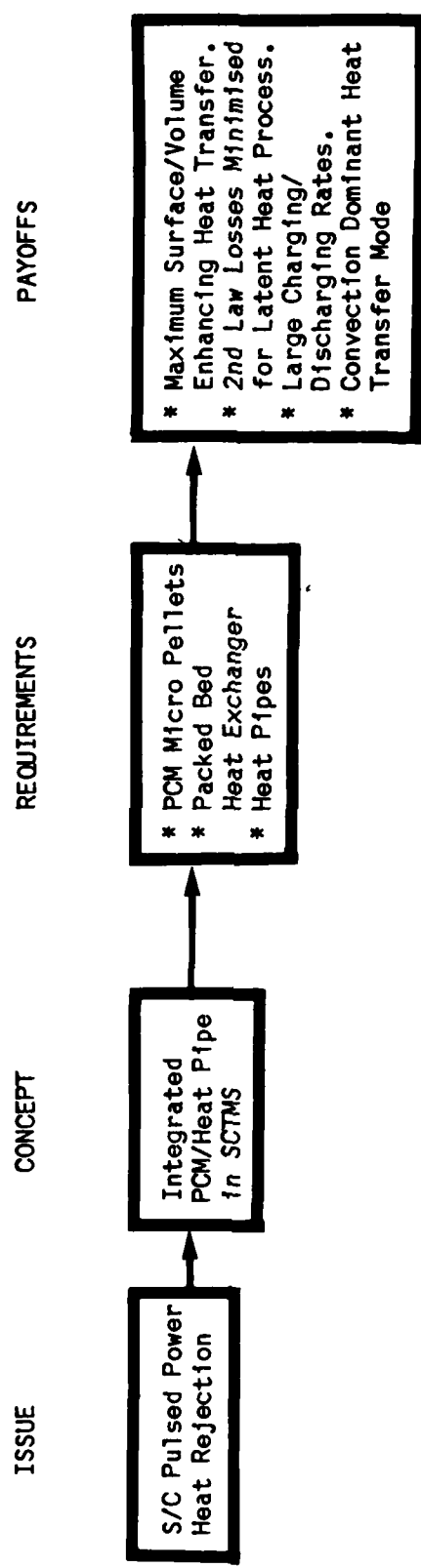
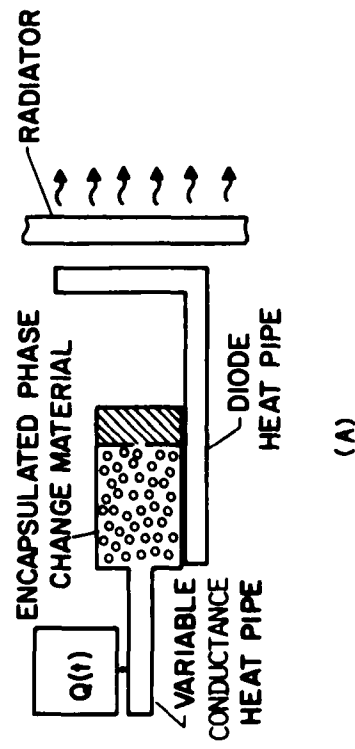


Figure 8. Design Aspects of the Proposed Concept



(A)

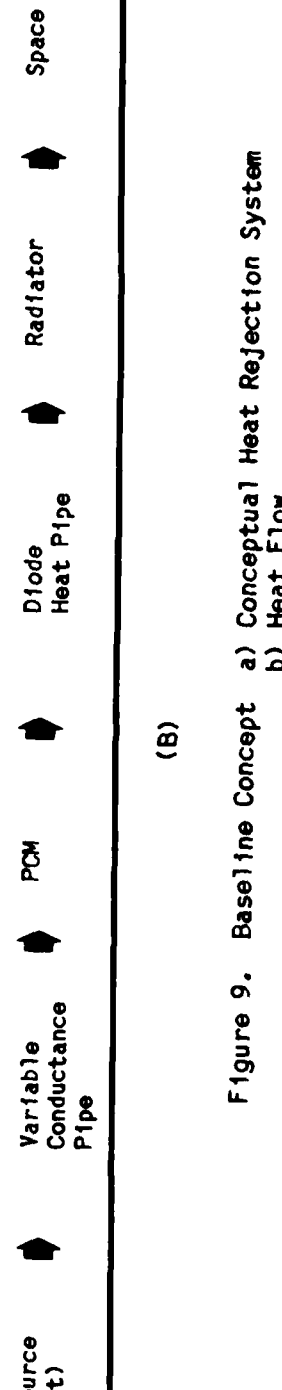


Figure 9. Baseline Concept
 a) Conceptual Heat Rejection System
 b) Heat Flow

heat transfer boundary conditions of the third kind were used at all of the boundaries. The energy equation for a component may be stated as the following:

The net rate of heat flow into a component through the boundaries is equal to the rate of increase of the internal energy of the component.

For the three-lump system, the energy balances for the three components respectively are as follows:

$$M_h C_h \frac{dT_h}{dt} = Q_h - Q_p \quad (\text{HEAT PIPE}) \quad [1]$$

$$M_p H_p \frac{dX}{dt} = Q_h - Q_p \quad (\text{PCM}) \quad [2]$$

$$M_r C_r \frac{dT_r}{dt} = Q_p - Q_r \quad (\text{RADIATOR}) \quad [3]$$

Here M is the mass of the component, C is the specific heat of the component, T is the temperature of the component, X is the melt fraction of the phase change material, t is the time variable, H is the latent heat of fusion of the phase change material, and the Q 's are the heat flow rates of the three components. The three heat flow rates are defined as follows:

$$Q_h(t) = U_h A_h (T_h(t) - T_p) \quad [4]$$

$$Q_r(t) = U_p A_p (T_p - T_r(t)) \quad [5]$$

$$Q_p(t) = U_r A_r (T_r(t) - T_s) \quad [6]$$

Here the 'U' parameters are the overall heat transfer coefficients for the three components, and the 'A' parameters are the associated areas of heat transfer of the three system components. Substituting Eqs. [4-6] into Eqs. [1-3] results in three linear, first order, ordinary differential equations for the transient variations of the temperature of the heat pipes, the melt fraction of the phase change material and the temperature of the radiators. The heat flow from the thermal bus is assumed to be a periodic function of time. For simplicity, a square wave function was selected as the periodic function. It can be shown that for the heat flow represented by a square wave that the ratio of the 'peak-to-average' heat flows is equal to one plus the

ratio of the 'off-to-on' time periods. For example, the 'peak-to-average' heat flow ratio for the special case of equal 'on' and 'off' is equal to two.

The reference masses of the three components of the thermal management system for the spacecraft are defined by the following expressions:

$$M_h = Q_h / G_h \quad [7]$$

$$M_p = Q_p n t_p / H \quad [8]$$

$$M_r = Q_r / G_r \quad [9]$$

Here the parameter 'tp' is the time of the peak heat load, the parameter 'n' is the number of peak time intervals, and the 'G' parameters are the specific weights of the components.

2. Thermal Management Subsystems' Models: The specific weights of the heat pipes and the radiators are evaluated at a peak-to-average heat flow of one, i.e. constant heat flow for the reference values. The effective, time-averaged, specific weights of the heat pipes and radiators can be calculated once the actual heat flows are obtained from the solutions of Eqs. [1-3]. The time-averaged specific weight of a heat pipe can be defined as the time-averaged heat flow divided by the mass of the heat pipe, and hence can be defined by the following expression:

$$G_{Ah} = Q_{Ah}/M_h = (Q_{Ah}/Q_A) G_h \quad [10]$$

Similarly, the time-averaged specific weight of a radiator can be defined as the time-averaged heat flow divided by the mass of the radiator, hence can be defined by the following expression:

$$G_{Ar} = Q_r/M_r = (Q_{Ar}/Q_A) G_r \quad [11]$$

The time-averaging is simply the time integral of the function divided by the time interval. The total mass of the thermal management system is the sum of the three components: the heat pipes, the PCM and the radiators.

3. Masses of the SCTMS Components

a. Heat Pipe: To determine the masses of the heat pipes in a SCTMS, a specific mass formulation is used.

$$dM_h = dN_h Q_h / G_h \quad [12]$$

where N_h is the number of heat pipes.

The total number of heat pipes can be calculated from the total heat load divided by the heat load of a single heat pipe, i.e.

$$dN_h = dQ_t / Q_h \quad [13]$$

The heat load of a single heat pipe can be calculated from the maximum heat pipe capacity divided by the maximum heat pipe length, i.e.

$$Q_h = CA_h / L_h \quad [14]$$

where CA_h = Capacity of the heat pipe.

L_h = Length of the heat pipe.

Combining Eqs. 12 and 13 yields

$$dM_h = dQ_t / G_h \quad [15]$$

The evaporator heat fluxes have constraints given by

$$q_e = Q_h / (L_e \pi D_h) \quad [16]$$

Thus combining with Eq. 14 yields the evaporator length

$$L_e = CA_h / (q_e L_h \pi D_h) \quad [17]$$

where L_e = Length of the evaporator.

D_e = Diameter of the heat pipe.

q_e = Heat flux of evaporator.

Similarly the condenser heat fluxes have limitations given by

$$q_c = Q_h / (L_c \pi D_h) \quad [18]$$

Thus combining with Eq. 14 yields the condenser length

$$L_c = CA_h / (q_c L_h \pi D_h) \quad [19]$$

q_c = Heat flux at the condenser.

L_c = Length of the condenser.

b. Phase Change Material: To determine the weight of phase change material in a SCTMS, a lumped mass representation is used, i.e.

$$H \frac{dM_p}{dt} = Q_p \quad [20]$$

where M_p = Mass of PCM

t = Time of storage

H = Latent heat of fusion

Q_p = Heat load of PCM

Solving the Eq. 20 for the differential mass of the PCM yields

$$\frac{dM_p}{dt} = Q_p / H \quad [21]$$

Since, the sensible heat storage of the PCM has been neglected, due to the dominate latent heat storage of the PCM the above equation is valid for limited cases for small Stefan numbers, i.e.

$$Ste = C_p \frac{dT_p}{H} \ll 1 \quad [22]$$

where C_p = Specific heat of PCM

dT_p = Temperature swing of PCM

H = Heat of fusion of PCM

In addition, the thermal resistance to conductive heat diffusion in the PCM is negligible in comparison to the overall coefficient of heat transfer between the PCM and the heat transport medium. Therefore Eq. 21 is valid for small Biot number, i.e.

$$Bi = U_p \Delta R_p / K_p \ll 1 \quad [23]$$

where U_p = Overall surface coefficient of heat transfer in the PCM heat exchanger

ΔR_p = Characteristic thickness of the PCM layer

K_p = Thermal conductivity of the PCM

c. Radiator: To determine the weight of the radiator in a SCTMS, two principles are used, a mass definition and a heat load definition, i.e.

$$dM_r = \rho_r L_r dA_r \quad [24]$$

and

$$dQ_r = q_r dA_r \quad [25]$$

where M_r = Mass of the radiator

Q_r = Heat load of the radiator

A_r = Radiative surface area

ρ_r = Mass density of the radiator

L_r = Characteristic thickness

q_r = Radiative heat flux

Substituting the differential area, dA_r , from Eq. 25 into Eq. 24 yields

$$dM_r = (\rho_r L_r / q_r) dQ_r \quad [26]$$

Multiplying and dividing Eq. 26 by the radiative surface area, A_r , yields

$$dM_r = dQ_r / (q_r A_r / \rho_r L_r A_r)$$

$$dM_r = dQ_r / (Q_r / M_r)$$

$$dM_r = dQ_r / (G_r) \quad [27]$$

Hence, if the specific weight of the radiator can be assumed to be a constant, then integrating Eq. 27 yields a linear relationship between radiator mass and thermal load, i.e.

$$M_r = Q_r / G_r \quad [28]$$

B. KNOWLEDGE-BASED SYSTEM

In the design of any knowledge-based system, one of the most difficult problems to be tackled is that of knowledge representation [14]. In order to first understand and then solve a problem, one must be able to represent the objects, relationships and the abstract concepts of the domain in the artificially intelligent system. Without proper representation it would be difficult to achieve a significant amount of intelligence in the program, as the crux of 'understanding' a problem is in abstracting it to a representation

which is complete and amenable to manipulation and transformation that leads to a solution. Therefore, the initial thrust of the present research is directed towards the development of appropriate representation. While addressing the representation and system design problems, full consideration is given to the state-of-the-art in the field of knowledge-based systems.

1. Automation of the Design Process: A typical design process of a SCTMS includes at least three distinct stages: a conceptual design stage, a development design stage and a design verification stage. In the conceptual design stage system tradeoffs are considered prior to selecting a preliminary design. The thermal design of SCTMS requires 'systems engineering' since a broad spectrum of technical disciplines are considered in this design process. As spacecraft systems grow in size, power and system complexity, the number of design options for SCTMS becomes enormous. Simple tradeoff studies only consider the interdependence of the various design parameters. Many current preliminary design processes only consider a single point design; however, automation of the preliminary design process would make it possible to consider total payload and mission requirements.

To assist in this design process, a knowledge-based system has been developed in 'Prolog'. This software serves as a design assistant for the development of SCTMS. The design assistant is implemented according to the suggestions found in [10]. These suggestions give the stages of operation and the levels of knowledge. The topmost level of the software determines an approximate design for the SCTMS. The lower levels then in turn refine the design, within their specific areas of expertise. Fig. 10 presents a flow chart of the overall system and Fig. 11 illustrates the stages of operation and the levels of knowledge required.

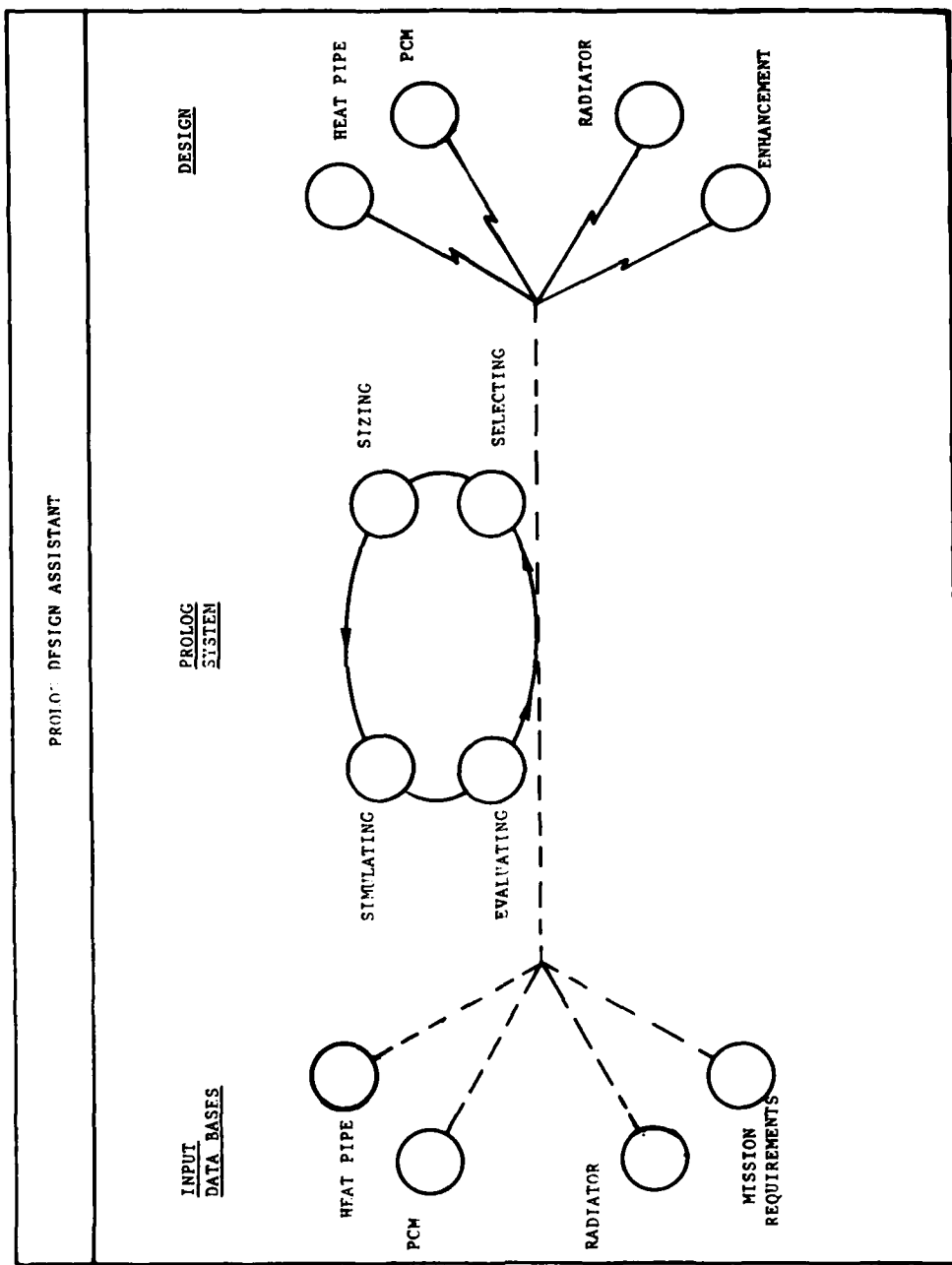


Figure 10. Design Assistant Flow Chart

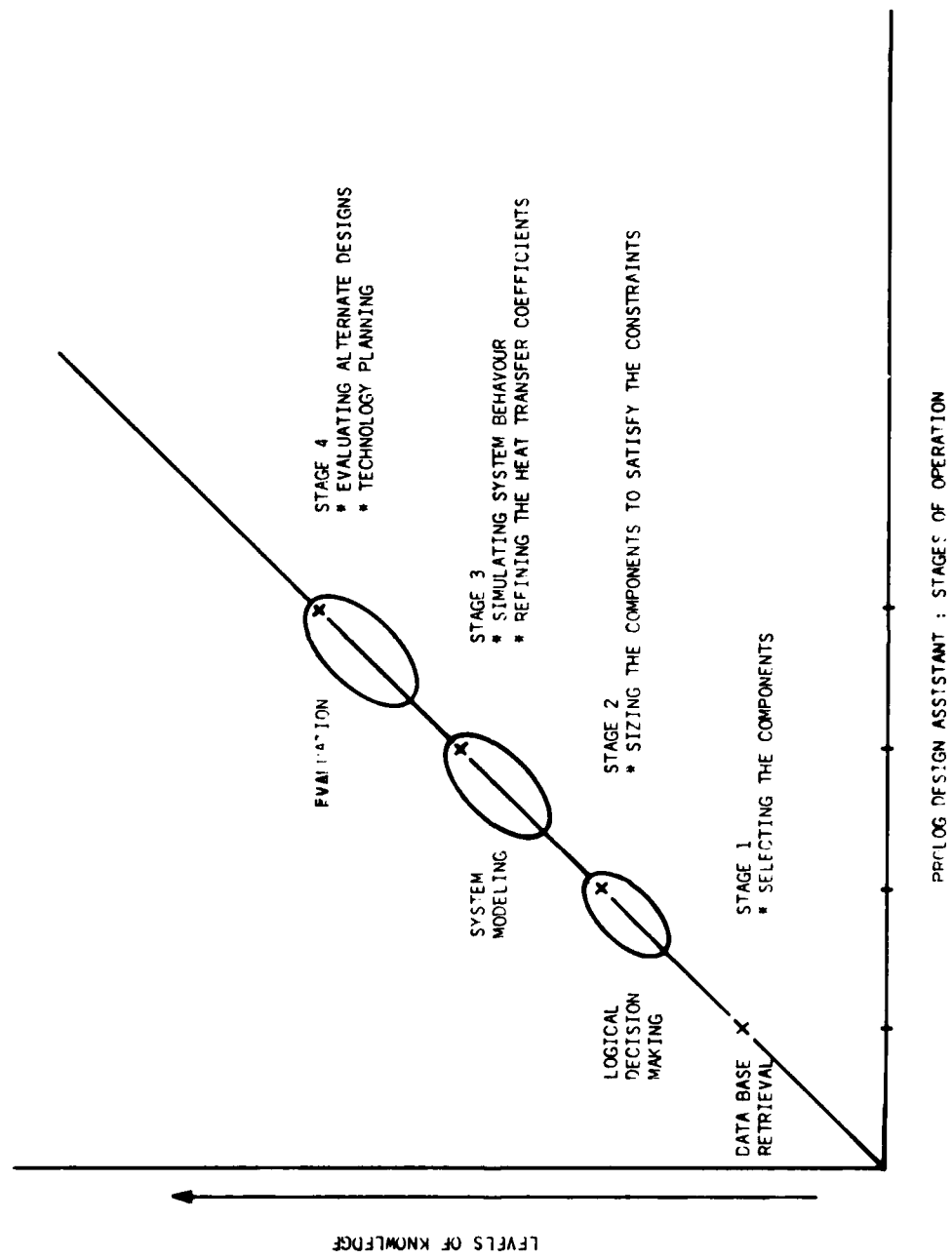


Figure 11. Design Assistant Levels of Knowledge

Specifically, the topmost level selects a PCM which is compatible with the initial temperature specifications and determines its size according to the mission requirements. This process is facilitated by the automatic search and selection capabilities of PROLOG. The second level of design is to select a heat-pipe, radiator combination which satisfies the given mass limit, yet has the required heat transfer capabilities. This combination heat pipe, PCM and radiator then serves as a candidate conceptual design.

Although the basic heat transfer capabilities of the selected components are matched, the actual behavior of the components in a pulsed power system may be very erratic. Hence, the third level of design is to simulate their behavior under the mission requirements, using the transient heat flow model described above, and to refine the overall heat transfer coefficients of the components so that the system behavior pulse after pulse, is bounded and predictable. The result is components: heat pipe, PCM and radiator, which together satisfy the basic mission requirements.

The final stage of the design is to determine the degree of enhancement (or relaxation) required to implement components with those heat transfer performance characteristics. In some cases of PCMs, heat transfer surface augmentation is necessary to compensate for relatively low thermal conductivity of the selected PCM. In other cases of PCMs, less stringent requirements of the overall heat transfer coefficient may allow for multi-configuration options.

2. Knowledge-Base: The knowledge-base of the design assistant has three partitions, Heat Pipe, PCMs, and Radiators. To build this knowledge-base an extensive literature survey covering topics of latent thermal energy storage systems and spacecraft thermal management systems was made. The bibliography was prepared with microcomputer software 'The Research Assistant' from Hi-Q

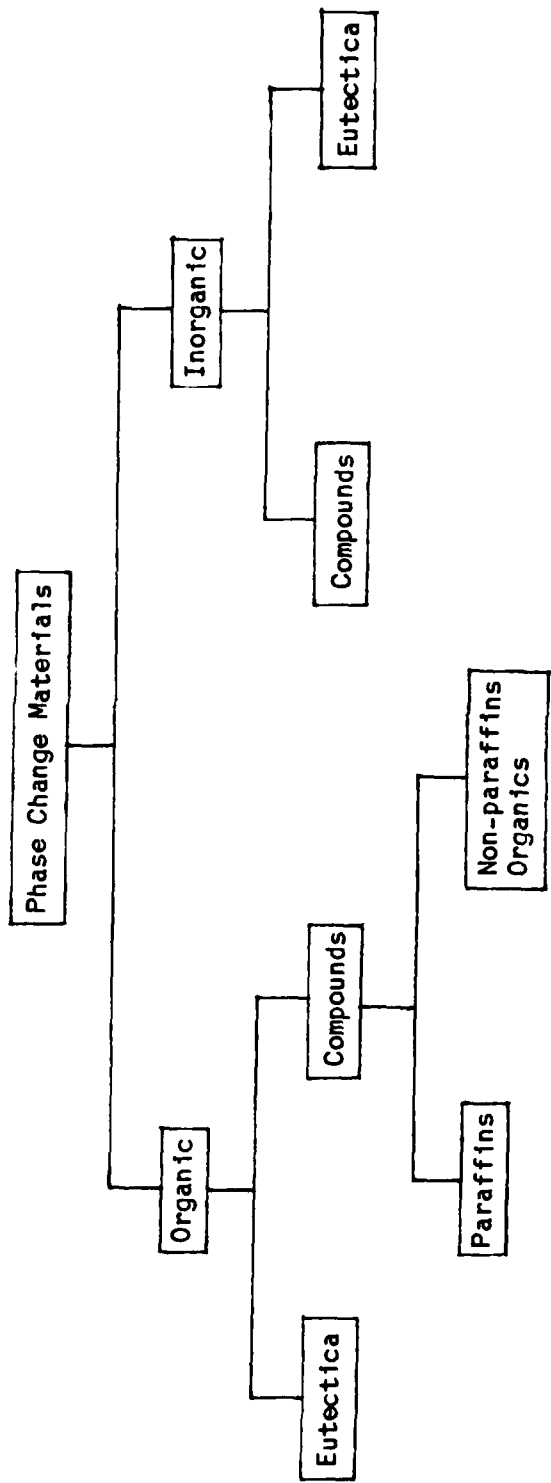


Figure 12. Family of Phase Change Materials

Table III. Desired Properties of PCMs

Criteria	Property	Comments
Thermodynamic	Melting point	Desired temperature
	Heat of fusion	High Latent Heat Fusion/unit Mass: small masses
	Density	High Density: small volumes
	Conductivity	Constant Density: small volume changes High Thermal Conductivity: small temperature gradients
	Supercooling	Minimum supercooling during freezing
Kinematic	Congruent Melting	Fixed temperature during phase change
	Stability	Stable: minimum chemical decomposition and separation
	Toxicity	Nontoxic: satisfies spacecraft environmental constraints
	Economic	Inexpensive and available in large quantities

Table IV. Phase Change Materials Considerations

1. Desired Material Properties
See Table III.
2. Candidate Heat Storage
Trade offs have to be made for PCMs in desired temperature range.
3. Melting and Freezing
Characteristics, supercooling of melt and stability to thermal cycling are important to the life of LHES system.
4. Thermal Cycling
The influence of thermal cycling on PCM characteristics must be measured experimentally. This affects the life of the LHES system.
5. Compatibility with
Materials of Construction
Knowledge of PCMs materials of regarding compatibility with conventional materials of construction is of particular importance of the assurance of the life of a LHES system.

(NAME) (CLASS) (TEMPERATURES °C)
(h_a - KJ / KG) (C_{p0} C_{p1} - KJ / KG / °C) (k_a k_b - W / M / °C)
(DENSITIES - KG / M³) (comment))

(polyethylene) (organic compound polymer) (132 132)
(184) (n-a n-a) (5.18 4.6)
(950 950) (solid-solid))

(polypropylene) (organic compound polymer) (166 166)
(66.9) (n-a n-a) (1.17 1.17)
(901 901) (solid-solid))

(polymethylene oxide) (organic compound polymer) (181 181)
(158.9) (n-a n-a) (2.3 2.3)
(1420 1420) (solid-solid))

(polyethylene oxide) (organic compound polymer) (57 57)
(94.5) (n-a n-a) (n-a n-a)
(1150 1150) (solid-solid))

(polyisoprene) (organic compound polymer) (32 35)
(27.8) (n-a n-a) (n-a n-a)
(n-a n-a) (solid-solid))

(85 % NaNO₃ - 8.8 % Na₂SO₄ - 5.7 % NaCl) (inorganic eutectic salt) (278 278)
(168) (n-a n-a) (0.78 0.78)
(2290 2290) (inexpensive))

(95.4 % NaNO₃ - 4.6 % NaCl) (inorganic eutectic salt) (297 297)
(178) (n-a n-a) (0.69 0.69)
(2260 2260) (inexpensive))

(69.9 % CaCl₂ - 30.1 % NaCl) (inorganic eutectic salt) (490 490)
(233) (n-a n-a) (4 4)
(2400 2400) (inexpensive))

(46.2 % KCl - 29.9 % CaCl₂ - 23.9 % NaCl) (inorganic eutectic salt) (515 515)
(265) (n-a n-a) (3.8 3.8)
(2160 2160) (inexpensive))

(79 % LiOH - 21 % LiF) (inorganic eutectic salt) (427 427)
(786) (n-a n-a) (2.6 2.6)
(1580 1580) (high-storage))

(LiOH) (inorganic compound salt) (460 460)
(874) (n-a n-a) (2.4 2.4)
(1430 1430) (high-storage))

(68 % KF - 32 % LiF) (inorganic eutectic salt) (492 492)
(523) (n-a n-a) (3.5 3.5)
(2520 2520) (high-storage))

Figure 13. PCM Database

(NAME) (CLASS) (TEMPERATURES °C)

(h_{∞} - KJ / KG) ($C_{p,\infty}$ $C_{p,1}$ - KJ / KG / °C) (k_{∞} k_1 - W / M / °C)
(DENSITIES - KG / M³) (comment))

(67.76 % Al - 27 % Cu - 5.25 % Si) (inorganic eutectic alloy) (524 524)
(308) (n-a n-a) (256 256)
(3300 3300) ()))

(66.8 % Al - 33.2 % Cu) (inorganic eutectic alloy) (548 548)
(275) (n-a n-a) (273 273)
(3510 3510) ()))

(82.1 % Al - 13.3 % Si - 4.6 % Mg) (inorganic eutectic alloy) (559 559)
(423) (n-a n-a) (199 199)
(2590 2590) ()))

(87.4 % Al - 12.6 % Si) (inorganic eutectic alloy) (577 577)
(431) (n-a n-a) (180 180)
(2661 2661) ()))

(octadecane) (organic compound other) (28 28)
(242.2) (2.18 2.18) (0.15 0.15)
(810 770) ()))

(lithium nitrate trihydrate) (inorganic compound hydrate) (30 30)
(296.5) (2.09 2.09) (0.5 0.5)
(1550 1430) ()))

(Na₂HPO₄ * 12 (H₂O)) (inorganic compound hydrate) (36 36)
(279.8) (1.67 1.93) (0.51 0.48)
(1520 1450) ()))

(myristic acid) (organic compound acid) (58 58)
(200.5) (1.59 2.26) (0.1 0.1)
(860 860) ()))

(cerrobend) (inorganic compound alloy) (70 70)
(33.4) (0.17 0.17) (18.8 18.8)
(9400 9200) ()))

(acetimide) (organic compound other) (81 81)
(242.2) (2.8 2.8) (0.25 0.25)
(1160 n-a) ()))

(CaCl₂ * 6 (H₂O)) (inorganic compound hydrate) (30 30)
(170.3) (n-a n-a) (108.73 50.97)
(1802 1562) (incongruent))

(Zn (NO₃)₂ * 6 (H₂O)) (inorganic compound hydrate) (36.1 36.1)
(133.9) (n-a n-a) (n-a 46.83)
(1937 1828) (expensive))

Figure 13. continued

(NAME) (CLASS) (TEMPERATURES °C)
(h_p - KJ / KG) (C_{p0} C_{p1} - KJ / KG / °C) (k_0 k_1 - W / M / °C)
(DENSITIES - KG / M³) (comment)))

(Ca (NO₃)₂ * 4 (H₂O)) (inorganic compound hydrate) (47.2 47.2)
(161.9) (n-a n-a) (n-a n-a)
(n-a n-a) ()))

(Mg (NO₃)₂ * 6 (H₂O)) (inorganic compound hydrate) (90 90)
(159) (n-a n-a) (61.5 48.95)
(1636 1550) (corrosive)))

(MgCl₂ * 6 (H₂O)) (inorganic compound hydrate) (115 115)
(164.9) (n-a n-a) (69.45 56.87)
(1569 1450) (corrosive)))

(wax suntech p116) (organic eutectic paraffin) (44 44)
(226) (2.95 2.51) (0.24 0.24)
(818 760) (nonmonotonic-conductivity)))

Figure 13. continued

Table V. Parameters Considered in the Analysis

- * Pressure drop through packed bed
- * Flow rate of HTF
- * Test section geometry
- * Total heat stored
- * Melt time
- * Effect of cycling
- * Convective heat transfer coefficient between HTF and PCM
- * Porosity

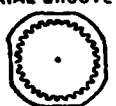
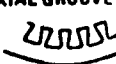
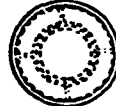
HEAT PIPE	FILM COEFFICIENTS W/cm ² - °C		TRANSPORT CAPACITY W-M (O-G)	RADIAL HEAT FLUX W/cm ²	
	EVAP	COND		UNIFORM	ONE-SIDED
CONVENTIONAL AXIAL GROOVE 	.68	.80	150	4.5	>2.6
RE-ENTRANT AXIAL GROOVE 	.74	.91	263	3.7	>3.0
SPIRAL ARTERY 	1.14	1.42	250	5.5	>3.9
PEDESTAL ARTERY 	1.14	1.42	250	5.7	
SLAB WICK 	1.14	1.42	191	5.7	

Figure 14. Proposed Heat Pipe Database

Microware, #8-13322, 102A Avenue, Surrey, B.C. Canada V3T 5J7. The literature is organized under three headings, SCTMS, latent thermal energy storage and phase change mathematical models.

a. Phase Change Materials Knowledge-Base: This consists of properties of about 50 selected PCMs. The PCMs are grouped into different classes as shown in the Fig. 12. The PCMs were selected keeping in view the desired properties shown in the Table III and IV. A sample PCM database is shown in the Fig. 13. The columns contain the name of the PCM, melting point, heat of fusion, thermal conductivity in solid state and liquid state, specific heat in solid state and liquid state and the last column contains comments with respect to PCMs considerations shown in the Table V.

b. Heat Pipe Knowledge-Base: At present, the heat pipe knowledge-base consists of single point database. The heat pipe is chosen according to the specific weight. The creation of a more complete heat pipe database will involve a greater effort due to its complex nature and all the factors involved are not known at this stage. Figure 14 gives some ideas in that direction. The implementation of a more complete knowledge-base for heat pipes may be performed as a future task.

c. Radiator Knowledge-Base: Here again, a single database is considered for the radiator knowledge-base. The radiator is selected according to the specific weight. Again, similar to the heat pipes, the creation of a more complete database for the radiator has been deferred to a future task.

IV. EXPERIMENTAL PROGRAM

As an ongoing research task, this report primarily addresses properties and thermal behavior of selected PCMs as candidates for possible use as thermal buffers of burst power conditions of SCTMS materials.

A. FUSIBLE PELLET CONCEPT

In the present concept, a packed bed of pellets can be designed to provide a specified thermal energy storage and charging/discharging rates. The two PCMs (Calcium choloride hexahydrate and high density polyethylene) selected for evaluation have the potential to satisfy the requirement of being impervious to water, the heat transfer fluid used in the experimental tests. In the case of the calcium chloride hexahydrate, the pellets or capsules are small, self-contained units in which the active core is separated from the water by organic resins making it impervious to the water. While in the case of the High Density PolyEthylene (HDPE), the PCM is non-porous and no coating or encapsulation is necessary.

The design and analysis of packed-bed heat exchangers require both thermophysical and geometric information, such as the porosity, device length-to-diameter ratio, and numerous thermodynamic properties of the thermal storage material. In a preliminary research task, some of these properties were obtained. Special attention was given to the HDPE because of its apparent unique characteristics. In the recent work on solid-solid PCMs, most of the effort has been directed at the solid-solid transition and how to produce the PCM, such as silanegrafted crosslinking or electron beam irradiation. Relatively little work has been devoted to the other properties of the material. However, few research teams have addressed the problems of the HDPE, such as its compressibility, relatively low thermal conductivity and compatibility with different heat transfer fluids [16-18].

B. HEAT TRANSFER EXPERIMENTS

The development of packed bed heat exchangers for SCTMS requires new technology. Emphasis is placed on developing a method for predicting the

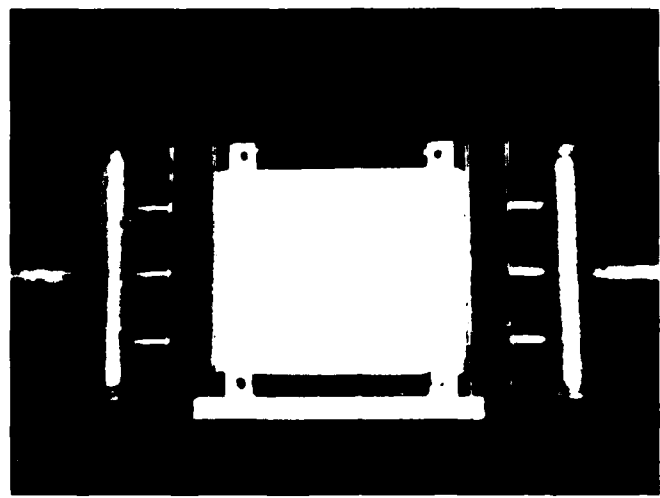


Figure 15. Heat Exchanger

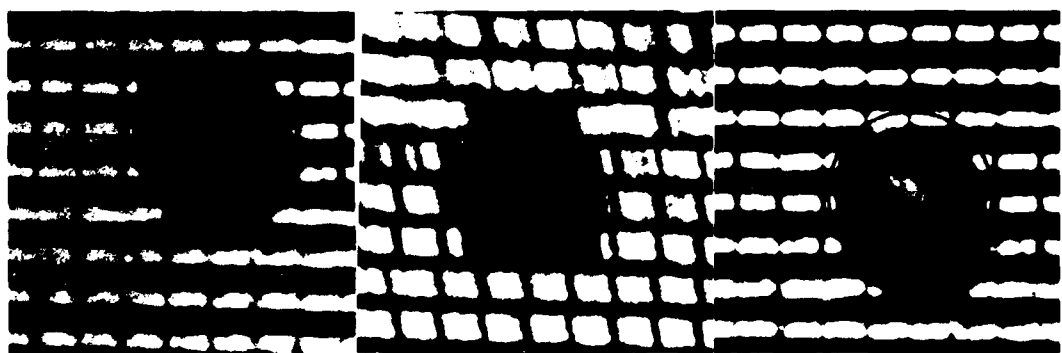


Figure 16. Phase Change of HDPE Pellet

thermal response of an entire packed bed heat exchanger unit rather than a single PCM pellet, in order to facilitate its design.

All of the existing latent heat storage devices use sensible heat transfer and suffer significant losses due to the Second Law of Thermodynamics. These losses can be minimized if a latent heat transfer process is used, i.e. a boiling and condensing heat transfer fluid. Hence the idea of a packed bed with a PCM integrated into the condenser in a heat pipe is promising. However, if one selects steam as the heat transfer fluid, several problems with PCMs have been observed such as pellet adhesion and moisture adsorption. For the crosslinked HDPE with a melting point of about 130 °C, ethylene glycol, silicone oil, water and steam have been tested. To test the process, the heat exchanger in Figure 15 was used. It consists of a rectangular cross section, stainless steel column to hold the pellets, and has a rectangular glass window on one side for photographic observation of the phase change phenomenon (Fig. 16). The design and analysis of packed bed heat exchanger requires both thermophysical and geometric information. Table V. shows the important parameters considered in the analysis. Both pressure drop and temperature measurements of the heat transfer fluid are being considered.

C. DESIGN ANALYSIS

In order to analyze the problem of using PCM pellets in a packed bed heat exchanger, several simplifying assumptions have been made. They are as follows:

- a. Heat transfer fluid properties are assumed constant,
- b. Heat transfer coefficient between the heat transfer fluid and the PCM is uniform in the heat exchanger,
- c. The mean velocity of the heat transfer fluid in the axial direction is constant,

- d. The axial conduction heat transfer between the pellets is negligible compared with the heat transfer via the fluid,
- e. The temperature distribution of the PCM is one-dimensional in the axial direction,
- f. The pellets are uniform in size and spherical in shape,
- g. The inlet temperature of the heat transfer fluid is constant.

The conservation of energy in the packed bed heat exchanger can be described by the following relationship between the time rate of change of the PCM and the convective coefficient of heat transfer:

$$h_c \Delta T A_s = dM_s/dt \quad H \quad [29]$$

where H = Enthalpy of the PCM.

Integrating with respect to time from the initial time of phase change to the time when one pellet has phase changed yields:

$$\tau = M_s H / (h_c \Delta T A_s) \quad [30]$$

To size the length of a packed bed heat exchanger, one can check the length that the fluid flows during the time for one pellet layer to melt. An expression can be obtained for this length as follows:

$$\delta = 4 \rho_s H D_s V / (6 h_c \Delta T \pi \epsilon D_p) \quad [31]$$

Following the analysis of T. Asahina and M. Kosaka [19], the pressure drop of the fluid passing through the packed bed can be obtained from the following expression:

$$\Delta p = (2 f \rho L V^2 / (g D_s A_{cs})) (1 - \epsilon) / \epsilon \quad [32]$$

where $f = 1.75 / Re^{0.1}$

and $Re = \rho D_s / \mu (4V / (D^2 (1 - \epsilon)^{2/3}))$

for $Re > 200$

Table VI gives several properties of the two PCMs pellets being experimentally investigated. The calcium chloride hexahydrate ($CaCl_2 \cdot 6H_2O$) material is being tested first in a rectangular cross section packed bed since

Table VI. Properties of PCM Pellets

PCM	HDPE	$\text{CaCl}_2 \cdot 6\text{H}_2\text{O}$
Melting Point, °C	125 - 140	27
Heat of Fusion, kJ/kg	210	147
Mass, kg	3.41×10^{-7}	1.87×10^{-3}
Diameter, m	4.0×10^{-3}	1.0×10^{-2}
Density, kg/m ³	914	1548

this arrangement allows for easy photographic recording of the phase change phenomena.

V. EXPERIMENTAL RESULTS

From an array of potential materials, two candidate PCMs in pellet form were selected for review: encapsulated calcium chloride hexahydrate and radiation-crosslinked high-density polyethylene (HDPE). The radiation cross-linking gives the HDPE the unique physical property of being self encapsulated. The HDPE can be heated to temperatures in excess of 150 °C without becoming entirely liquid. The individual pellets of HDPE are form-stable. Recent studies [15] have shown that the HDPE pellets of retain their shape; however, pellets do tend to stick together. Lane's recent book [16] on latent heat storage materials gives an excellent and comprehensive review of both of these materials.

In order to study the direct contact heat transfer between the form-stable HDPE or the encapsulated $\text{CaCl}_2 \cdot 6\text{H}_2\text{O}$ and the heat transfer fluid, several material properties were needed for the design of the packed bed heat exchanger including the porosity, the pellet microhardness (Vickers Hardness Number), the melting temperature and the recrystallization temperature.

A recent investigation [17] has shown that HDPE has a melting point in the temperature range of 125-140 °C and values for latent heat as high as 210 kJ/kg which we have confirmed experimentally. HDPE melts and freezes reversibly and congruently. Thus the value of heat of fusion remains at a constant value even after repeated cycling 36 through the melting point. HDPE changes from white opaque crystalline solid to a clear transparent viscoelastic liquid phase. A finely divided white residue was observed to be present at the bottom of the flask when heated to a temperature higher than the melting point in a bath of water or oil. It has been observed [18] that

HDPE pellets which are exposed to a dose of about 8 megarads adhere to one another at their point of contact, but the packed bed of pellets maintain its open porous structure throughout the thermal cycling phase.

1. Porosity and Density: The porosity of the packed bed heat exchanger was calculated from experimental measurements of the HDPE and calcium chloride hexahydrates. The pellets were poured into a calibrated glass cylinder while varying packing pressure was axially applied with a dead-weight system. The resulting packing pressure was measured on a calibrated load cell with an analog readout. Water was added to the packed bed and measured to determine the void volume as a function of both bed temperature and packing pressure. The temperature of the packed bed in the cylinder was maintained by a small tape heater. In addition, a microhardness tester was used to determine the hardness of the HDPE as a function of radial location in the pellet. During the cross-sectioning of an encapsulated bed of HDPE for the microhardness test, a small void in the center core of each pellet was discovered. Hence, the mass density of the hollow pellets was also calculated from experimental measurements of the HDPE to be $914. \text{kg/m}^3$. To eliminate any initializing effect of the applied packing pressure, multiple loading/unloading cycles were made until consistent values of porosity were obtained. Table VII gives the calculated values of the porosity for the HDPE as a function of packing pressure and bed temperature. Table VIII gives the calculated values of the porosity for calcium chloride hexahydrate as a function of packing pressure at the melting temperature.

Table VII. HDPE Porosity versus Temperature and Pressure

Packing Pressure [kPa]	Bed Temperature in degrees centigrade			
	60	80	100	120
103.4	0.3386	0.3400	0.3428	0.3370
155.1	0.3371	0.3386	0.3410	0.3342
106.8	0.3355	0.3368	0.3382	0.3329
258.5	0.3340	0.3350	0.3361	0.3312

Table VIII. $\text{CaCl}_2 \cdot 6\text{H}_2\text{O}$ Porosity versus Pressure

Packing Pressure [kPa]	Bed Temperature = 27 degrees centigrade
	Porosity
0	0.4822
103.4	0.4800
258.5	0.4772

2. Photographic Observations: An array of nine HDPE pellets was attached to an Aluminum block (0.057 m x 0.057 m x 0.006 m) having a fine grid (0.0013 m) machined on the surface. Two 400 watt cartridge heaters were placed in two holes drilled into the side of the aluminum block. Photographs of the HDPE pellets were taken at temperatures ranging from 117 to 175 $^{\circ}\text{C}$. From negatives (0.10 m x 0.13 m) of the photographs, enlarged prints (0.20 m x 0.26 m) of the pellets were made to determine the variation of size and shape with respect to temperature. The resulting prints also showed that during the phase change process the HDPE pellets changed from opaque to transparent. The nominal

diameter of the pellets was measured to be approximately 0.004 m. Figure 16 shows three different temperature conditions of a single pellet. The right photograph has a circle superimposed around the pellet illustrating the variation from an idealized spherical shape. The middle photograph shows the same pellet during the phase change with an opaque center and a transparent outer shell. The left photograph in Fig. 16 illustrates a transparent pellet after complete phase change has occurred. The photographs were taken with a Calumet 4 x 5 with double bellows extension. The lens was a F4.8/0.216 m Ilex. The shutter speed range was 1 to 1/150 sec and F-stop range was 4.8 to 45. The lighting was accomplished with two 3800 K photo spot lights. The photographs were taken at 1/8 sec and F16 with a resulting 1.2 to 1 ratio of the negative to original length. The film selected was an ASA 50 Polaroid positive/negative 4 x 5 land film.

Several other characteristics of the HDPE pellets in their so-called 'form-stable' liquid phase were observed. A pellet at 175°C was squeezed by a pair of hand tweezers. The pellet was noted to be soft and pliable and showed a strong tendency to adhere to the metal tweezers. This adhesion property was reconfirmed in Fig. 17 which shows a packed bed of pellets having undergone cyclic heating and packing in a graduated cylinder during a porosity test. The pellets clearly adhere to each other even when heated in a bath of oil.

3. HDPE Pellet Microhardness: A Leitz MINILOAD-Hardness Test, equipped with a square Vickers pyramid indenter, was used to measure the hardness of the crosslinked HDPE at various radial locations on numerous sectioned pellets encapsulated in a hard resin. The Vickers hardness number is defined as the load divided by the area of contact from the indenter. The results of 16 different measurements showed that the Vickers hardness number varied from 5.8 to 9.5 kg/mm². These results indicate that the crosslinked HDPE is a very soft



Figure 17. Cylinder of HDPE after Multiple Phase Change Cycling

material in comparison to metals. The general trend of the tests indicated that the material is harder near the center core and becomes softer near the outer surface.

The microhardness testing was restricted to the HDPE pellets since the salt hydrates undergo a normal phase change process with the liquid being encapsulated in a flexible spherical shell.

4. HDPE Pellet Differential Thermal Analysis Results: To determine the melting and the recrystallization temperatures, a thermogalvanometry-differential thermal analysis (TG-DTA) was performed. The TG-DTA was originally the only technique available. Its capability is limited to detection of phase transitions and chemical reactions. The TG-DTA is not to be confused with the Thermogravimetric analysis (TGA) used for composition and thermal stability studies. Several random samples of the pellets were used. The results indicate that the melting temperature of the crosslinked HDPE is approximately 130 °C and the recrystallization temperature is approximately 120 °C. Differential scanning calorimetry (DSC) results would have allowed specific heats of the crosslinked HDPE to be measured. However due to nonavailability of a DSC at this facilities, the specific heats were not determined. Others [17] have recently reported such results for crosslinked HDPE. It should be noted that the values from the DSC are dependent on the thermal history due to the nature of polymers. Hence, one might conclude that actual test of prototype packed bed heat exchangers are necessary. Hence, actual testing of a prototype packed bed heat exchanger is planned for several PCM's.

5. Parametric Studies: Figures 18-21 give the results of a parametric study of the pressure drop as a function of the ratio of the length to

diameter of the packed bed. A set of lines for constant diameters are drawn for a fixed volumetric flow rate of the heat transfer fluid resulting in constant Reynolds number lines. Water was selected as the heat transfer fluid in the calculations. In the case of cylindrical packed beds of HDPE, one can see in Fig. 18 that for a Reynolds number equal to 289 and a length to diameter ratio of 6 that the pressure drop would be approximately 26 kPa. Likewise for a $\text{CaCl}_2 \cdot 6\text{H}_2\text{O}$ filled cylindrical packed bed, one can see in Fig. 19 that for a Reynolds number equal to 294 and a length to diameter ratio of 6 that the pressure drop would be approximately 2.3 kPa. In the case of a rectangular cross section packed bed heat exchanger, Fig. 20 and 21 illustrate the relationship between the pressure drop and the length to hydraulic diameter ratio for HDPE and $\text{CaCl}_2 \cdot 6\text{H}_2\text{O}$, respectively. It is evident from Eq. 31

$$\delta = 4 \rho_s H D_s V / (6 h_c \Delta T \pi \epsilon D_p),$$

that the pellet diameter along with the porosity influence the pressure drop across the packed bed heat exchanger.

6. Thermal Analysis: Thermal analysis of a packed bed of $\text{CaCl}_2 \cdot 6\text{H}_2\text{O}$ in pellet form was performed. Water was chosen for the Heat Transfer Fluid (HTF) as it is clear, abundantly available, has suitable properties and is inexpensive. For this experimental application (see Fig. 22), the availability of low pressure steam and tap water enabled a variety of flow and temperature conditions to be obtained by proper mixing. The storage unit instrumentation consisted of a paddle wheel flowmeter, weight tank, a thermometer, two pressure gages and eight thermocouples. The paddle wheel flowmeter and weight tank was used to measure the water flow rate and thermocouples measured temperatures at various locations in the storage unit. These were used to determine whether the PCM was charged or discharged at the

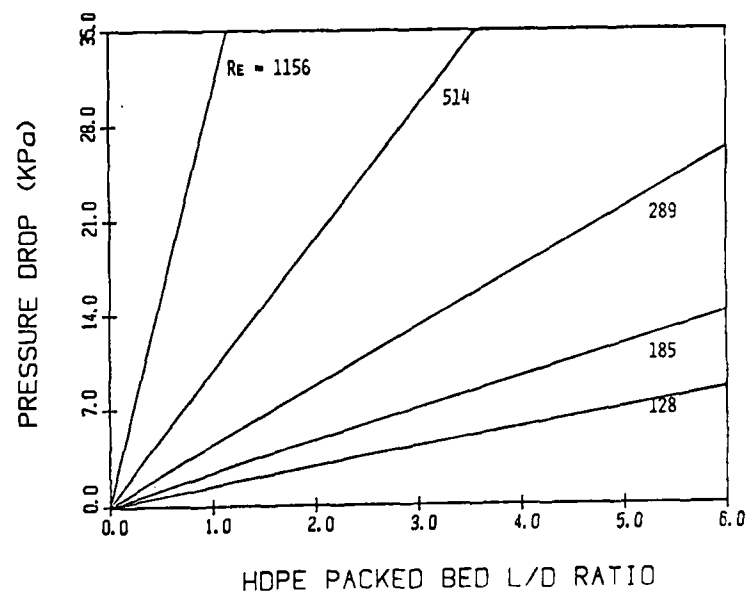


Figure 18. Pressure Drop vs. L/D Ratio for Cylindrical Bed of HDPE

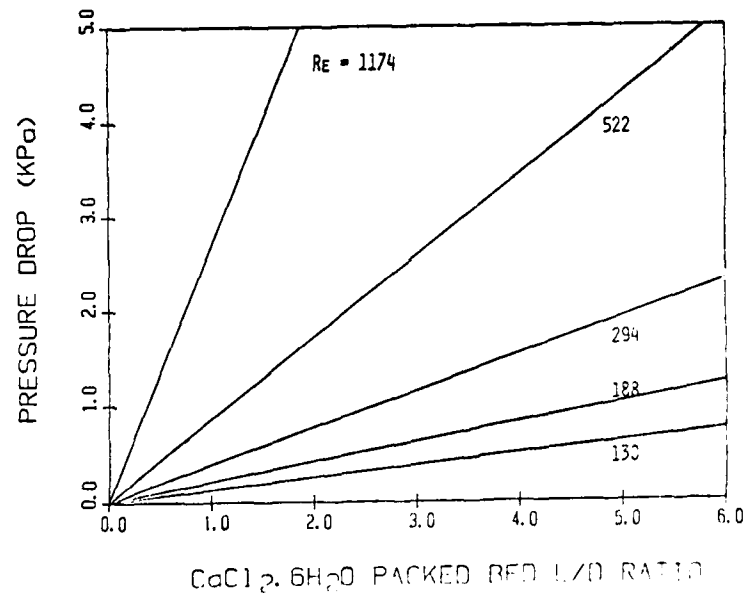


Figure 19. Pressure Drop vs. L/D Ratio for Cylindrical Bed of $\text{CaCl}_2 \cdot 6\text{H}_2\text{O}$

beginning of each test and to obtain a qualitative understanding of the thawing or freezing process.

Tests were conducted for both charging and discharging of the PCM. Prior to starting each test, the PCM was cooled or heated so that it was completely frozen for charging tests and melted for discharging tests. The temperature of the PCM was verified by reading the thermocouples to ensure that all PCM temperature readings were at least 3⁰F below the melting point for charging process and 3⁰F above the melting point for discharging process.

Six test runs were performed, three charging and three discharging, with water flow rates of 0.2, 0.4 and 0.6 gallon per minute. The test conditions were established by operating the steam mixing valves and the valve on the water line. The data acquisition for discharging process began once all the thermocouples readings were approximately 84⁰F. The inlet HTF temperature was lowered to approximately 76⁰F by shutting off the steam and the temperatures and flow rates were recorded at an interval of 30 seconds until the discharging process was completed. Figures 23, 24 and 25 show the temperature vs. time curves for the mass flow rates 0.2, 0.3 and 0.4 gpm. For the three mass flow rates the outlet temperature lags behind in inlet temperature, showing that the PCM is discharging heat. It is difficult to measure the time required to melt the PCM, as the heat capacity of the heat exchanger is far greater than the latent heat of PCM. Hence the response of the PCM packed bed cannot be accurately determined. A steady state analysis cannot be performed since it is difficult to lower the inlet water temperature from 86⁰F to 76⁰F instantaneously with the present setup. A transient analysis was performed to approximately calculate the mass of PCM discharged vs. time for different mass flow rates using the following equation.

Considering an energy balance at any instant of time, the heat absorbed by the water plus the heat lost to the surrounding due to natural convection

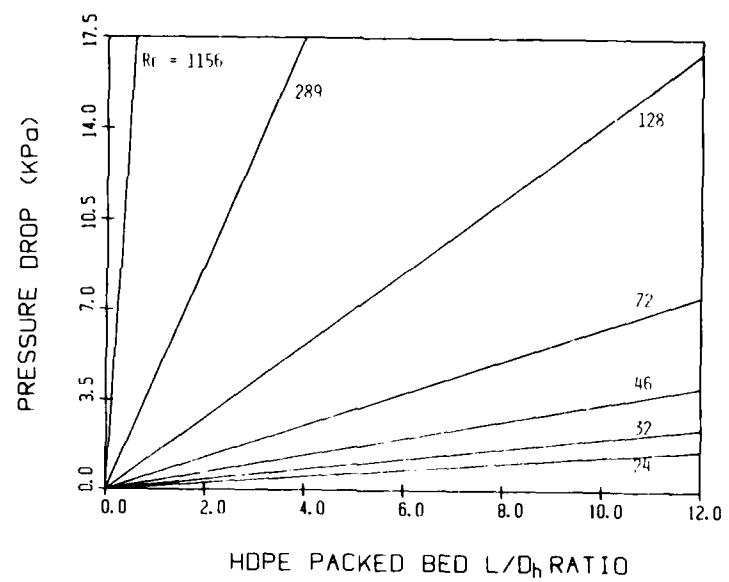


Figure 20. Pressure Drop vs. L/D Ratio for Rectangular Bed of HDPE

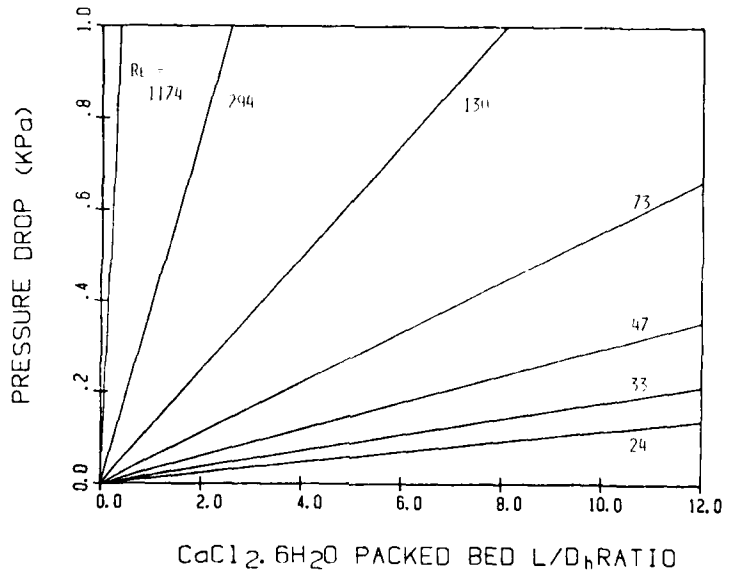


Figure 21. Pressure Drop vs. L/D Ratio for Rectangular Bed of $\text{CaCl}_2 \cdot 6\text{H}_2\text{O}$

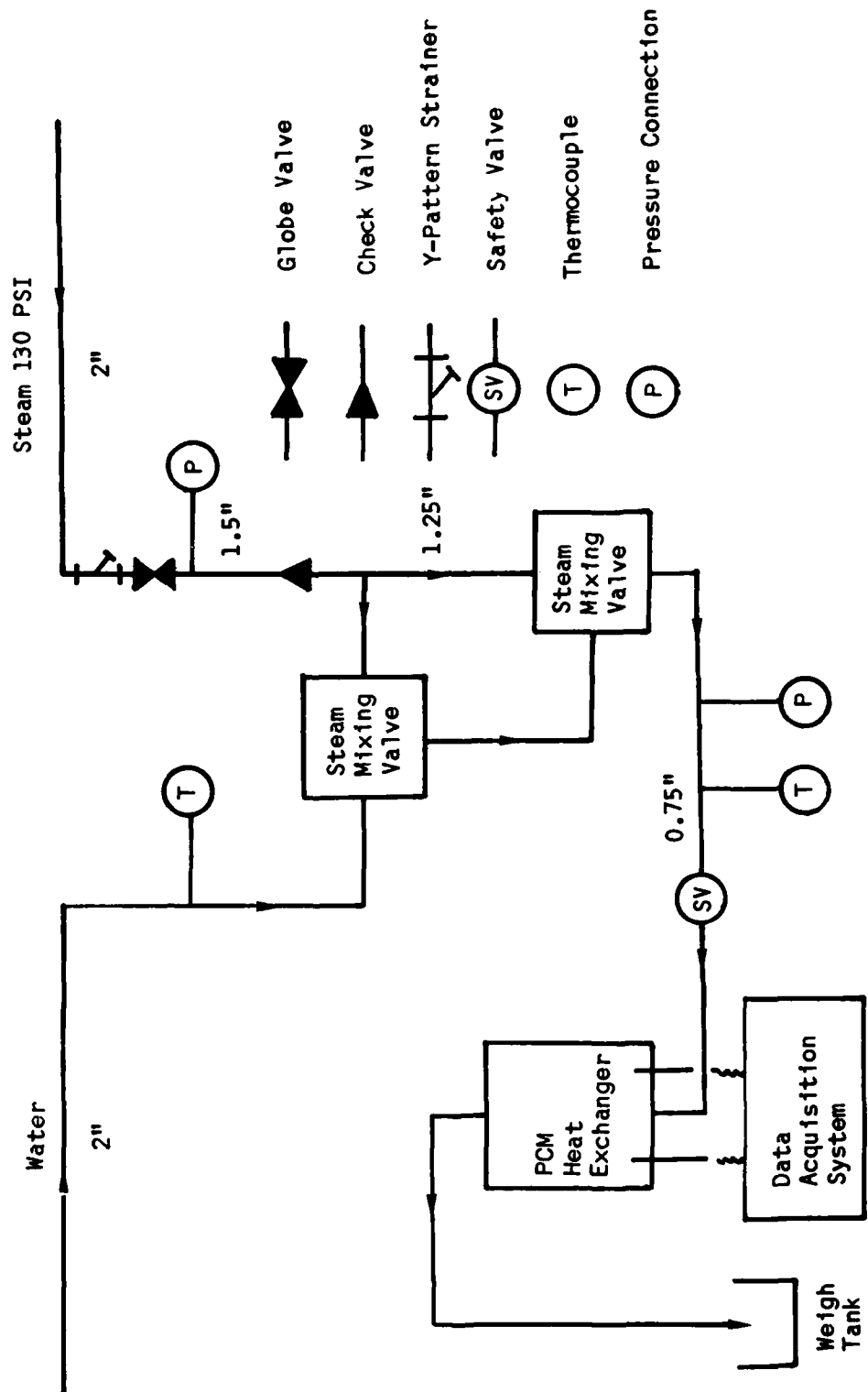


Figure 228. Present Experimental Setup

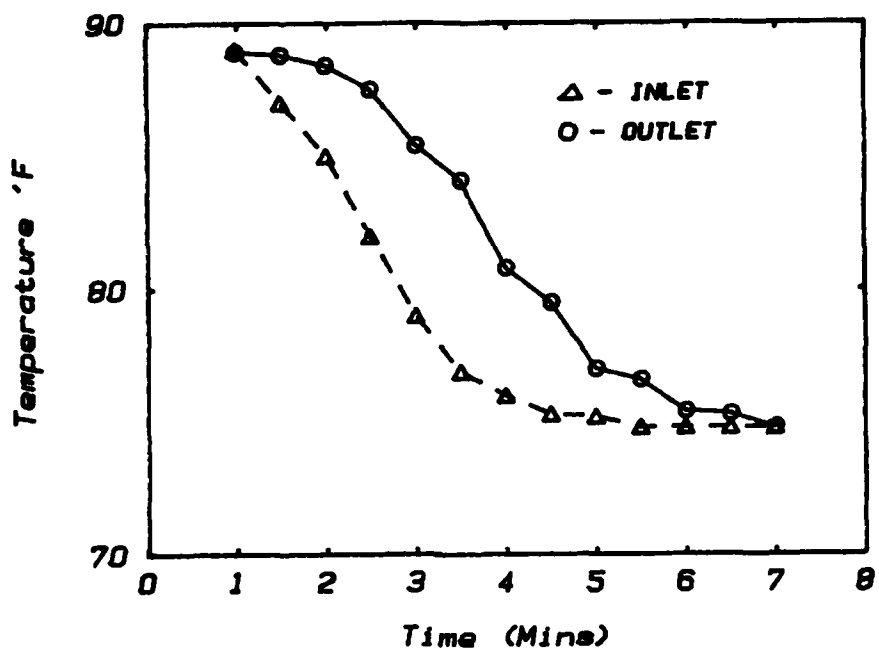


Figure 23. Fluid Temperature vs. Time
for Flow Rate of 0.2 gpm

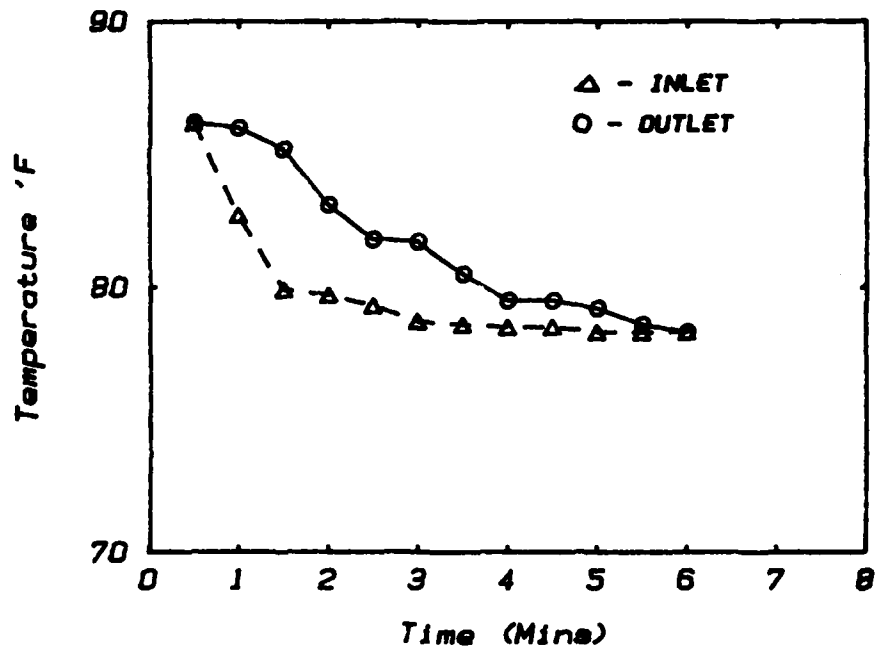


Figure 24. Fluid Temperature vs. Time
for Flow Rate of 0.3 gpm

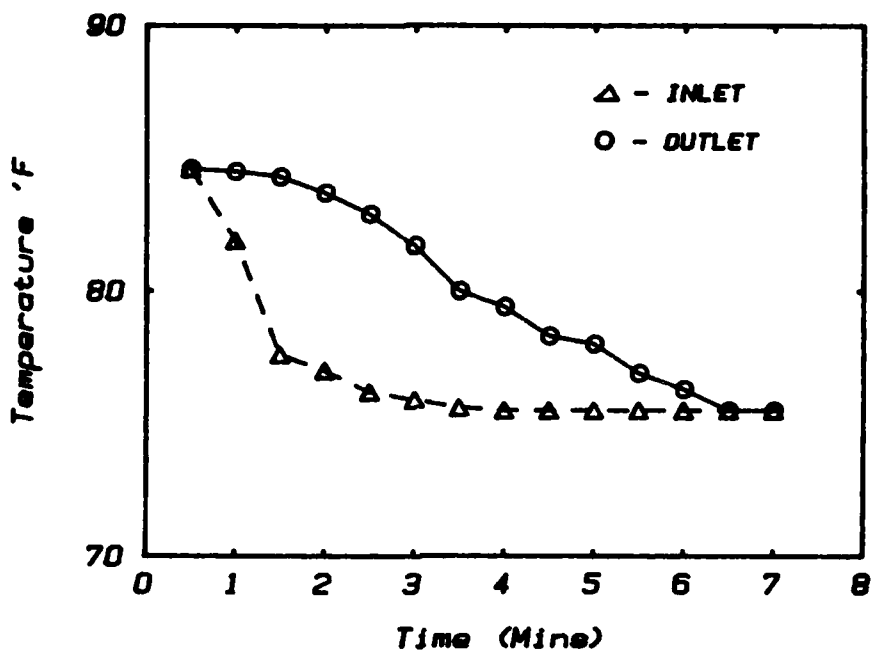


Figure 25. Fluid Temperature vs. Time Curves for Flow Rate of 0.4 gpm

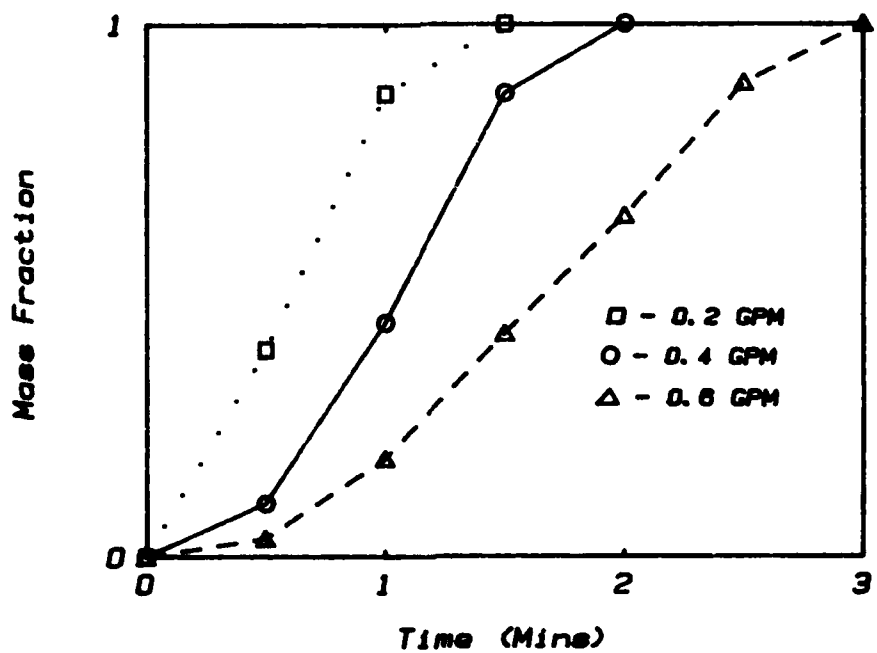


Figure 25. Mass Fraction vs. Time Curves for Different Flow Rates

equals the heat discharged by the PCM,

$$\text{i.e. } \int_0^{\tau} \dot{m}_{\text{water}} C_p (T_{\text{out}} - T_{\text{in}}) dt + \int_0^{\tau} h A (T_{\text{box}} - T_{\text{sur}}) dt \\ = m_p X(\tau) H$$

where \dot{m}_{water} = mass flow rate of water

m_p = mass of PCM

X = fraction of PCM melted

T_{out} = outlet water temperature

T_{in} = inlet water temperature

h = film coefficient of water

A = surface area of the heat exchanger

T_{box} = temperature of the surface of the heat exchanger,

i.e. $(T_{\text{in}} + T_{\text{out}}) / 2.0$

T_{sur} = ambient temperature

τ = time

The sensible heat contribution is small compared with the latent heat of the PCM. Figure 26 shows mass fraction vs time curves for different flow rates. The time required for discharging the PCM increases as the flow rate drops. These results should be used only as a guide to future experimental work. Some recommendations for future experimental work are discussed in the next section.

VI. CONCLUSIONS AND RECOMMENDATIONS

The application of phase change materials for thermal buffering of temperature sensitive equipment from pulsed heat loads of future SCTMS appears to satisfy the objectives. The initial selection of the candidate materials might be ranked on latent heat of fusion, however, the final selection should will not be based solely on a maximized latent heat of fusion. The specific weights of radiator and the heat pipes are operationally dependent on numerous parameters. Novel heat pipe and radiator designs will be required to achieve the desired performance.

The results of this preliminary investigation of the PCMs for SCTMS have been presented to identify the feasibility and capabilities of the selected PCMs for thermal buffers in fusible pellet concept. Several technical issues relating to the thermophysical properties were evaluated to determine the design improvements for the experimental facilities. The highly crystalline polymers such as radiation crosslinked, high density polyethylene show potential for a direct heat transfer process between a boiling/condensing heat transfer fluid and a PCM due to its rather unique property of self encapsulation. Further experimental verification of the bulk thermophysical properties of pelletized PCMs in the packed bed form is needed. Also methods to avoid adhesion of HDPE pellets at temperature up to 150°C for packed bed conditions are needed.

The results of the thermal analysis of the PCM storage unit recommends an altogether new experimental set up. The proposed experimental setup is shown in Fig. 27. It consists of the following:

- a. High temperature bath
- b. Bypass valves
- c. Air cooler
- d. Thermocouples
- e. PCM heat exchanger
- f. Micro-computer data acquisition system

By having this arrangement the following problems associated with the current setup are resolved.

- a. Control of the input fluid temperature.
- b. Sensible heat of the heat exchanger minimized.
- c. Fluid leakage.
- d. Lower fluid pressures in the system by using oil as HTF for higher temperature approximately instead of steam.

The prototype design assistant satisfies our initial expectations. It properly selects, sizes, and refines the components for a three component SCTMS model. Our next goal is to install a larger database of components and mission requirements and to exercise the software over a larger set of design problems.

Two interesting extensions of this work are possible. The first is to extend this work horizontally: to develop a family of design assistants, each tailored to a specific type of design problem, continuous power, very high power pulsed systems, pulsed systems with very short cycle time, etc. These separate assistants could then be called by a supervisory process which would determine from the mission requirements which assistant should be consulted. The second extension would be vertical: to develop additional levels to the present assistant which would further refine the physical dimensions and structural characteristics of a three component SCTMS.

A very interesting prospect, from an AI perspective, is the possibility of capturing the knowledge of SCTMS design, as it is acquired by the researchers themselves, documenting it, implementing it, and preserving it in a body of software. Hence with a working prototype in hand, the most important phase of AI work begins. A significant amount of domain specific

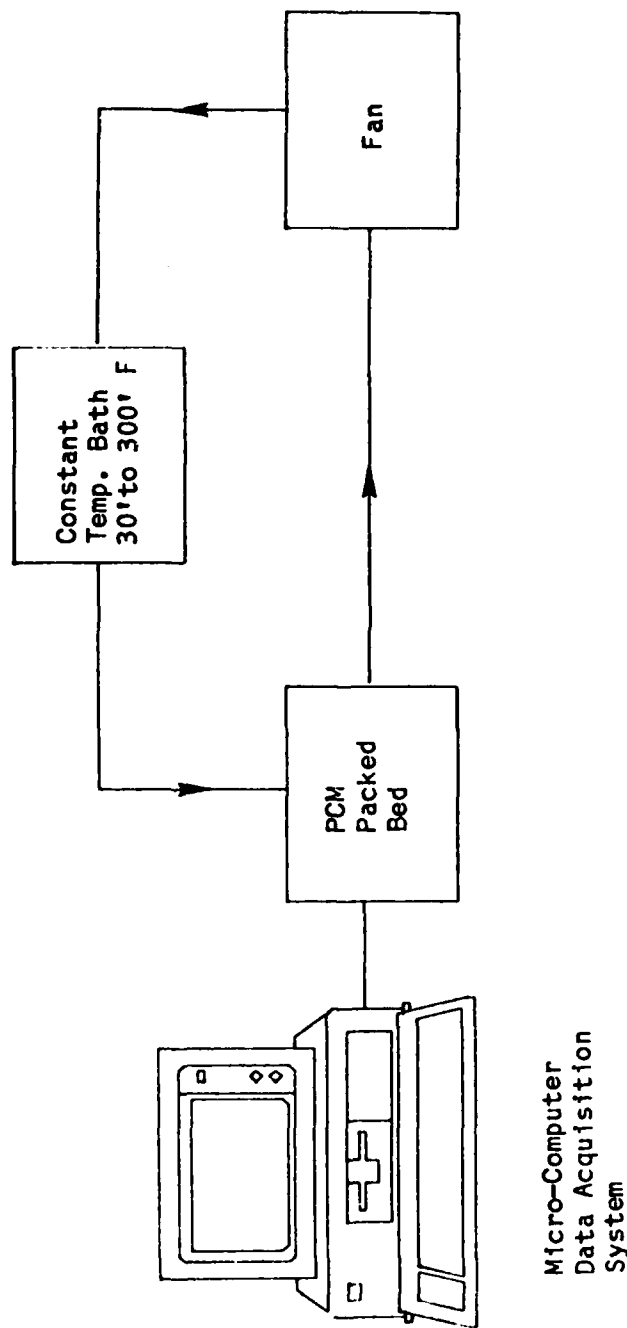


Figure 27. Proposed Experimental Setup

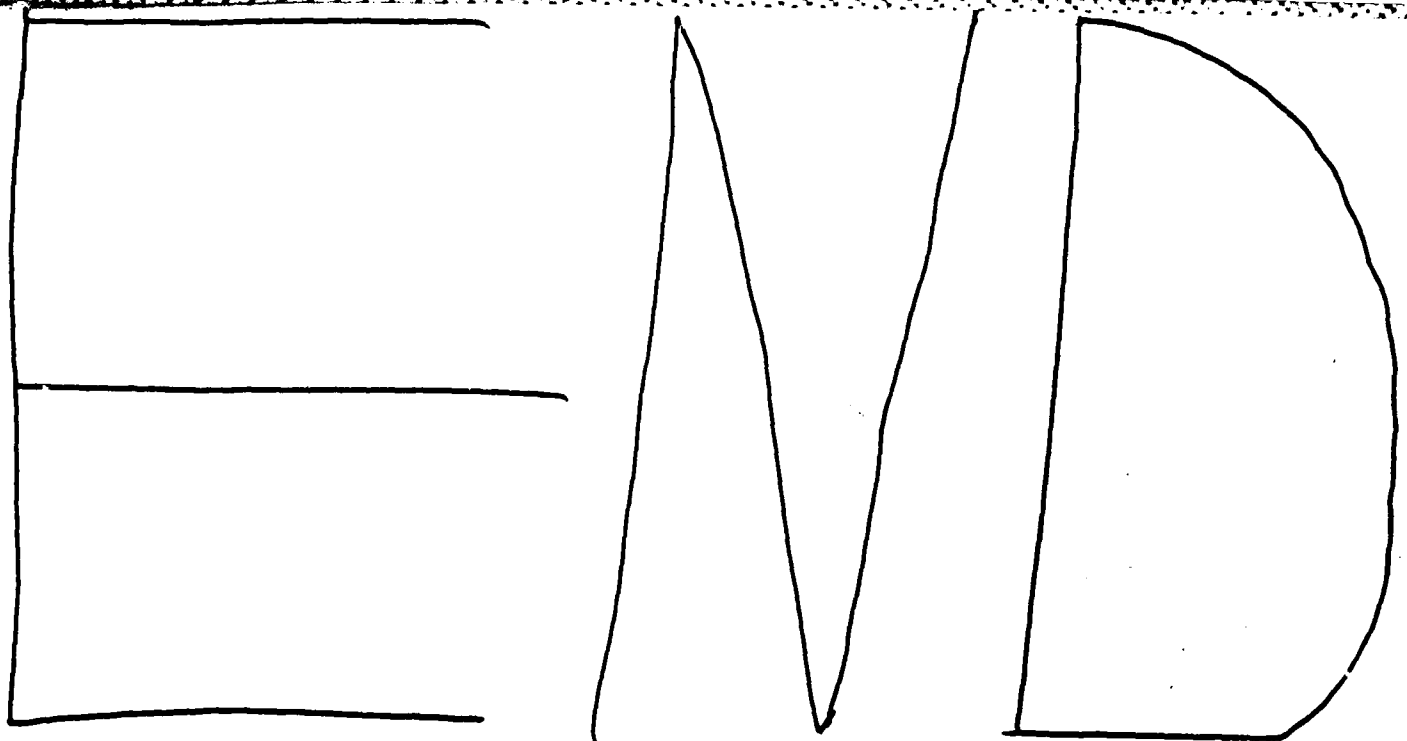
knowledge has been captured in a few lines of executable code. The task now is to give that knowledge a more general representation and to implement the tools that can in turn apply knowledge in a more general setting.

BIBLIOGRAPHY

1. B. Harwell and F. Edelstein, Advanced Thermal Control Techniques for Emerging Communications Satellites , AIAA 19th Thermophysics Conference, AIAA paper no. 84-1774, Snowmass, CO, June 1984.
2. S. Z. Fixler, Satellite Thermal Control Using Phase-Change Materials , J. Spacecraft, vol. 3, no. 9, pp. 1362-1368, 1966.
3. J. W. Sheffield and V. J. Van Griethuysen, Weight Characteristics of Future Spacecraft Thermal Management Systems , AIAA 22nd Aerospace Sciences Meeting, AIAA paper 84-0054, Reno, NV, January, 1984.
4. J. W. Sheffield, R. P. Kher and V. J. Van Griethuysen, Phase Change Materials for Spacecraft Thermal Management , Proceedings of the 19th IECEC, San Francisco, CA, vol. 1, pp. 152-157, Paper No. 849113, 1984.
5. Takao Ishimoto and Leroy M. Herold, Spacecraft Thermal Control: The management of energy transfer , Quest Magazine, vol. 5, no. 1, 1981, TRW Inc.
6. J. W. Sheffield, Weight Characteristics of Future Spacecraft Thermal Management Systems , Final Report AFWAL-TR-84-2005, AF Wright Aeronautical Laboratories, February 1984.
7. MICRO-PROLOG 3.1, Logic Programming Associates Ltd. 10 Burntwood Close, London SW18 3JU, England, March 1984.
8. Angelo Ferraro, George Yenetch, Robert Haslett and Robert Kosson, Thermal Energy Storage Heat Exchanger , Grumman Report, pp. 4.52-4.63, 1980.
9. A. Abhat, Short Term Thermal Energy Storage , Review Physics Applications, vol. 15, pp. 477-501, 1980.

10. D. C. Brown and B. Chandrasekaran, An Approach to Expert Systems for Mechanical Design , IEEE Trends and Applications Conference, Gaithersburg, MD, May 1983.
11. K. G. Kempf, Manufacturing and Artificial Intelligence , ECCAI Conference on Artificial Intelligence: Towards Practical Application, Zurich, April 1984, North Holland, T. Bernold and G. Albers (eds).
12. B. R. Fox, L. T. Brewster, R. P. Kher, J. W. Sheffield and Valerie J. Van Griethuysen, Design Assistant for Spacecraft Thermal Management System , Proceedings of the 20th IECES, Miami Beach, FL, vol. 1, pp. 1.425-1.429, paper no. 859398, 1985.
13. M. N. Ozisik, Basic Heat Transfer, pp. 113, McGraw-Hill Book Company, New York, 1977.
14. Ajay Sharma and W. J. Minkowycz, Knowtran: An Artificial Intelligence System for Solving Heat Transfer Problems , Int. J. Heat Mass Transfer, vol. 25, no. 9, pp. 1279-1289, 1982.
15. R. L. Cole, Thermal Storage Device Based on High-Density Polyethylene , Interim Progress Report ANL-83-52, Argonne National Laboratory, June 1983.
16. G. A. Lane, Solar Heat Storage: Latent Heat Materials, vol. 1, CRC Press, Inc., 1983.
17. M. Kamimoto, Y. Abe, S. Sawata, T. Tani, and T. Ozawa, Development of Latent Heat Storage Unit Using Form-Stable High Density Polyethylene for Solar Total Energy Systems , pp. 1790, 18th IECEC, Orlando, FL, August, 1983
18. J. E. Davision and I. O. Salyer, Electron Beam Irradiation of High Density Polyethylene Pellets for Thermal Energy Storage , Final Report ORNL/Sub-7641/1, Oak Ridge National Laboratory, May 1983.

19. T. Asahina and M. Kosaka, A Thermal Storage Analysis on Packed Bed
of Alumina Spheres , Proceedings of Int. Solar Energy Society
Congress, pp. 537-540, New Delhi, India, January 1978.



12-86

